Storrun vindpark – validering av modellers orografiska effektivitet

Orografisk effektivitet – validering av flödesmodeller

Förberett	Rémi Gandoin, 21 december 2011
Kontrollerat	textwise.dk
Accepterat	Thomas Krogh (KROGH)
Godkänt	Thomas Krogh (KROGH)

Dok.nr.	1116826
Ver.nr.	0
Ärendenr.	200-09-0411

Innehållsförteckning

1. Introduktion

17 maj 2011

1.1 Storrun-vindparken

Storrun-vindparken är belägen i Sverige. Den består av 12 Nordex N90-vindkraftverk på 2,5 MW. Se en översikt i figuren nedan:

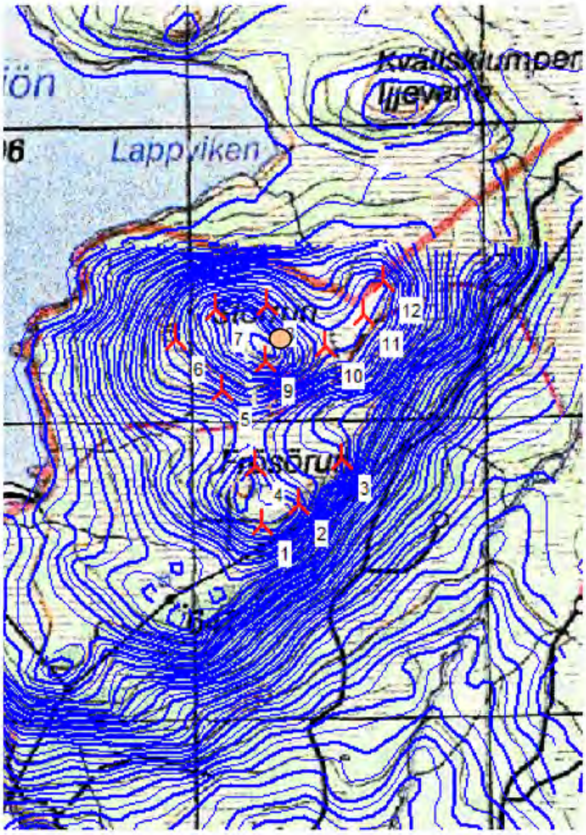

Terrängen kan klassificeras som halvkomplex. Höjdskillnaden varierar mellan 660 och 740 m i vindparksområdet (2×2 km). Bilder finns i bilagan. Höjden modelleras med hjälp av konturlinjer i 5-metersintervall.

Bedömningen av vindresurser baseras på en 3-årsmätning med en 50-metersmast som är placerad i den norra delen av vindparken (den orange punkten i figuren ovan).

Vindklimatet i området beskrivs nedan. Starka vindar kommer vanligtvis från vindriktningssektorerna 300° och 330°.

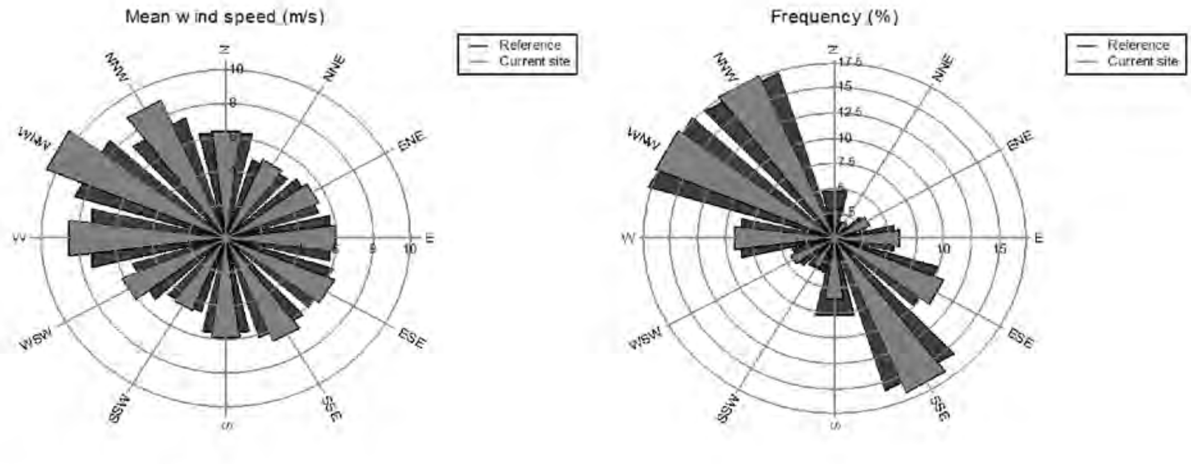

1.2 Modeller

DE har ombetts att jämföra resultaten från en mesoskalmodell (MIUU) med den vedertagna flödesmodellen i branschen, WAsP, som implementerats i WindPRO 2.7. MIUU beskrivs i [1]. En jämförande beskrivning av modellerna finns i tabellen nedan:

	WAsP	MIUU
Tidsavhängig	Nej	Ja
Turbulensmodell	Linjär	Mesoskala
Använder värden från mast på plats	Ja	Nej
Horisontell upplösning	Ned till 2 m	100 och 300 m
Vertikal upplösning	Resultat var 5:e m	8 nivåer logaritmiskt fördelade mellan 0 och 100 m

1.3 Mätvärden (vind och produktion)

Modellerna jämförs endast med produktionsdata, eftersom jämförelsen mellan MIUU och mastvärden redan har utförts i [1]. SCADA-data från vindparken har gjorts tillgängliga och omfattar en period på 2 år (2009–2011).

1.4 Jämförelsemetod

Från SCADA-databasen: 10-minutersvärden för effekt [kW], vindhastighet i nav [m/s], vindriktning i nav [deg], girvinkel [deg]. Data har filtrerats för tillgänglighet.

Målet med den här studien är att jämföra båda modellerna vad gäller orografisk effektivitet, i syfte att förstå hur respektive modell kan användas i komplex terräng. Det är självklart att det slutliga resultatet för respektive modell, det vill säga produktionen i varje vindkraftverk, måste jämföras med mätdata. Inga ytterligare justeringar har utförts och därför har analysen följande begränsningar:

- Ingen justering per vindhastighetsmätare: alla vindhastigheter ingår, eftersom den orografiska accelerationen antas vara vindhastigheten oberoende av flödesmodell.

- Ingen direkt jämförelse med de absoluta siffrorna över årlig energiproduktion, endast de relativa produktionssiffrorna anges.
- Vakmodellering ingår inte i analysen, eftersom det inte är ett resultat av flödesmodellerna. För de fyra huvudsakliga vindriktningarna har de friströmmande vindkraftverken valts ut, vilket innebär 4 testobjekt. Se figuren nedan:

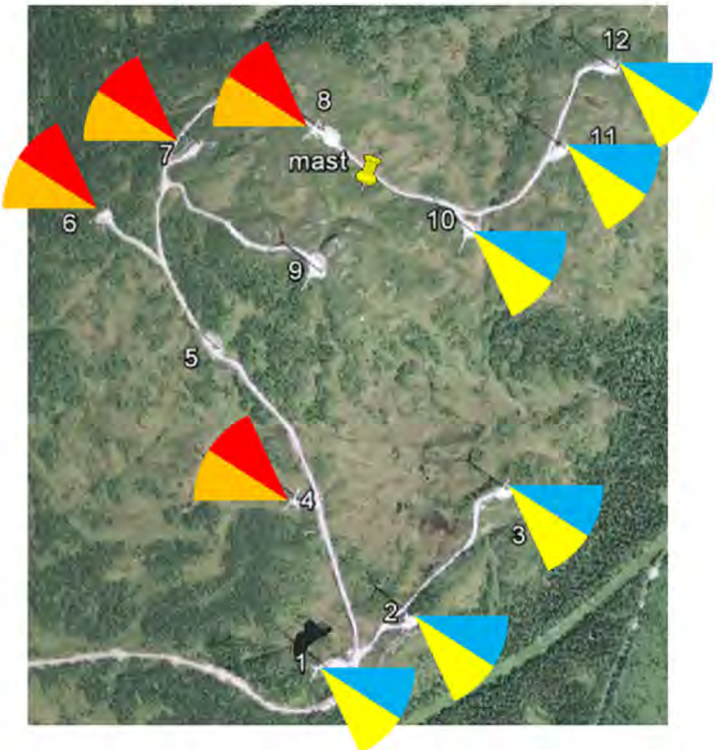

WAsP har används i WindPRO 2.7 och som indata används vindstatistik som uppmätts vid masten, orografi och ytjämnhetslinjer.

Rutnät på 100 och 300 m för vindresurser på navhöjd med Weibull-statistik över vindparksområdet har tillhandahållits DE och har använts som indata för beräkningen.

2. Resultat och diskussion

Den uppmätta normaliserade effekten för vart och ett av de 4 testobjekten anges i figuren nedan. De två grå fälten är resultaten från de två olika SCADA-databaserna som är tillgängliga.

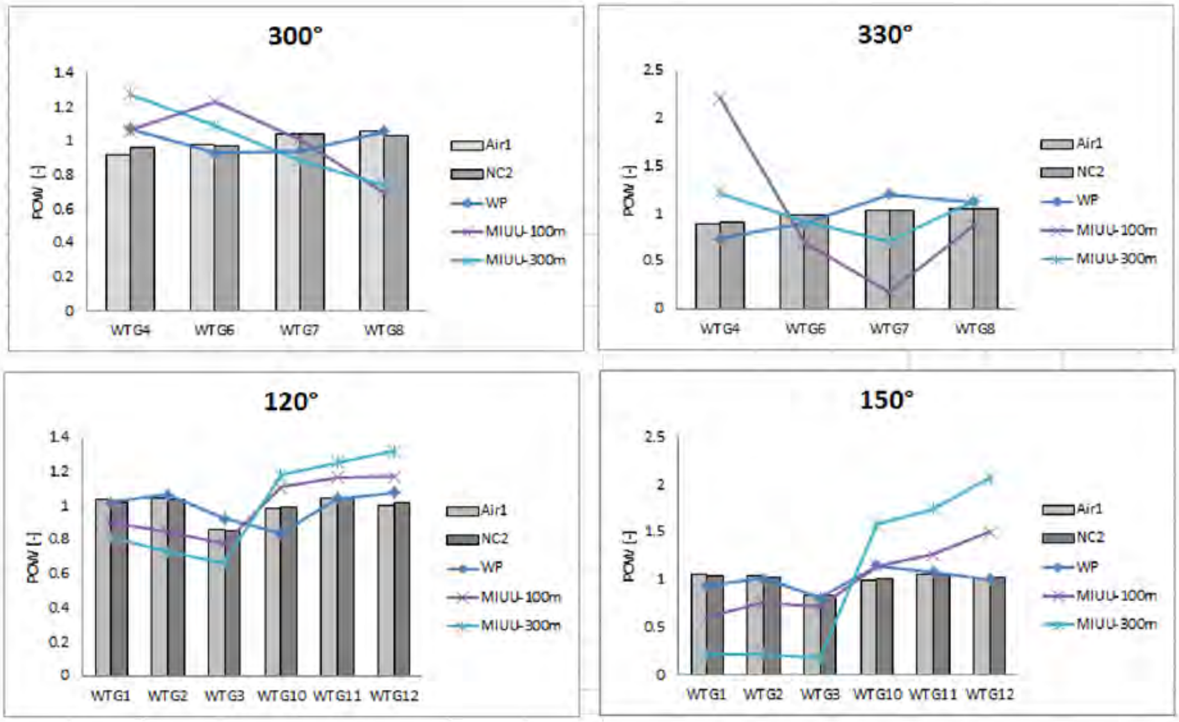

För det första kan man notera att den relativa skillnaden i produktionen inte överskrider 10 %, och att den för det mesta ligger inom 5 %. Osäkerheten i effektkurvan är cirka 3 % och därmed når denna jämförelse gränsen för godtagbar osäkerhet.

För det andra ligger WAsP alltid närmare mätvärdena och avläser trenden för riktningarna 120 och 150 grader mycket väl.

För det tredje kan man notera att MIUU vid 100 m är närmare än MIUU vid 300 m, men några tydliga skillnader i mätvärden uppvisas.

3. Sammanfattning och framtida arbete

Några få slutsatser kan dras från analysen:

- Två olika databaser med två olika vindhastighetsvärden och årsperioder visar liknande resultat vilket ger tillförlitlighet i mätningarna.
- WAsP visar sig avläsa trenden och den relativa skillnaden i effekt mellan vindkraftverken väl.
- Användningen av mesoskala i komplex terräng medför en mycket hög osäkerhet. Eftersom den inte modellerar atmosfärisk turbulens i de lägsta skikten bör den kombineras med en mikroskalmodell.

Bilaga

AN ESTIMATE OF THE WIND POTENTIAL OVER STORRUN USING THE MIUU-MODEL

Hans Bergström
UPPSALA 2010-11-01

1 Introduction

The use of meso-scale models for wind resource assessments has increased during resent years. Especially in complex terrain, the need for more advanced models than has earlier been used is often obvious. Also observations of offshore winds over the Baltic Sea show complexity and in-homogeneity to a much larger extent than are often expected regarding offshore winds.

Results with a higher-order closure meso-scale model, (the MIUU-model developed at the Department of Meteorology, Uppsala University), show that with this type of model the observed complex and inhomogeneous wind fields also turn up in the model results. A higher-order closure model is, however, computer-time consuming to run, why care has to be taken to limit the number of model runs needed as much as possible.

A method to simulate the climatological wind field using the MIUU model has been developed at Uppsala University, reducing the total number of simulations needed. With this method a limited number of climatologically relevant simulations are performed, with different wind and temperature conditions, and a weighting based on climatological data for the geostrophic wind (horizontal pressure gradient) is made in order to finally estimate the wind climate. The method is applicable for mapping the wind resources with a resolution of 0.5-10 km. To use this method geostrophic wind (strength and direction), sea and land temperatures, topography, roughness, and land use are needed. No observed boundary-layer winds are needed other than for verification. Comparisons between model results and measurements show good agreement.

2 The MIUU-model

The MIUU-model is a three-dimensional hydrostatic meso-scale model, which has been developed at the Department of Meteorology, Uppsala University, Sweden, (Enger, 1990). The model has prognostic equations for wind, temperature, humidity and turbulent kinetic energy. Turbulence is parameterised using a level 2.5 scheme following Mellor and Yamada, (1974). The closure is described in detail in Andrén (1990). The MIUU model has a terrain-influenced coordinate system (Pielke, 1984), roughly following the terrain close to the surface and gradually transforming to horizontal at the model top. To reduce influences from the boundaries, the modelled area is chosen to be much larger than the area of interest. This also makes it possible to account for effects of, for instance, mountains and water areas which are outside the investigated area, but which may anyhow be of importance to the wind field within the area of interest. To limit the number of horizontal grid points, a telescopic grid is often used, with the highest resolution only in the area of interest. In the vertical, the lower levels are log spaced while the higher levels are linearly spaced. The lowest grid point is at height z_0, where z_0 is the roughness length, and the model top is typically at 10000 m. Commonly 8 levels are used in the model up to 100 m height.

At the lower boundary, roughness length and altitude (of land) have to be specified at each grid point. Topography is taken from digitised maps from Lantmäteriet with a resolution of 50 m. The roughness over land has been divided into classes according to land cover. Land cover data is taken from Lantmäteriet with a resolution of 25 m. During winter, the roughness length is set to 0.001 m over open terrain to represent snow-covered land areas. Also temperature has to be given or estimated at the lower boundary for each grid point. The land surface temperature, and its daily and monthly variation, is estimated with a surface energy balance routine using as input solar radiation and land use. Over sea the observed monthly average sea-surface temperatures have been used.

The MIUU model has been used earlier in many case studies in different types of landscapes, showing good agreement with observations. In Källstrand et al. (2000) the Baltic Sea offshore wind field is investigated. The model has also been used studying winds and boundary layer turbulence structure along the west coast of USA (Söderberg and Tjernström 2001; Söderberg and Tjernström 2002; Brooks et al. 2003). Simulations with the MIUU model in mountainous terrain have been done, for example around Lake Mohave in the Colorado River Valley (Enger et al. 1993, Koracin and Enger, 1994). Wind climate investigations have been made for a mountain area in northern Sweden (Bergström and Källstrand, 2000 and 2001). In Bergström (1996) and Sandström (1997) the MIUU-model has been used to simulate the climatological wind field over the Baltic Sea. Bergström (2002) gives a general description on modelling the wind climate using a higher-order closure model like the MIUU-model, and in Bergström (2003) some tests are presented regarding the sensitivity of the resulting wind climate on the choice of model runs used for the final climatological weighting.

3 Model domain

To include effects on the wind climate from areas outside Storrun, model runs with 5 km resolution were first made covering the whole of Scandinavia, including also the Baltic States. The results from the 5 km runs were then used to give values at the lateral boundaries of 1 km resolution model domains. The 1 km model runs were 'nested' into the 5 km model domain. In doing this account could be taken of topography and land-sea differences on a larger scale which may still affect the local wind climate in smaller areas of specific interest. 1 km resolution results are available for the whole of Sweden as the result of the National Wind Resource Mapping (Bergström and Söderberg, 2009).

The resolution was further increased over the Storrun area in two steps. First from 1 km to 300 m, and finally from 300 m to 100 m. For the 300 m model runs 111 x 111 grid points were used, covering an area of 63 km x 63 km with 300 m resolution in an area of 20 km x 20 km and 2 km distance between the two outermost grid points. For the 100 m model runs 131 x 131 grid points were used, covering a 30 km x 30 km area. The 100 m resolution here covered an area of 8 km x 8 km and the distance between the two outermost grid points were 1 km. To minimize effects of the lateral model boundaries upon the results a region with expanding grid spacing was used in an about 20 km and 10 km wide strip around the area with 300 m and 100 m grid distances respectively. Maps of the interpolated topography (0.09 and 0.01 km^2 resolution) used in the model calculations are shown in Figure 1 and Figure 2. The corresponding roughness lengths are shown in Figure 3 and Figure 4.

In the vertical there were 29 grid points. The first one is at the height z_0, where z_0 is the roughness length. Close to the ground the vertical grid points are logarithmically separated in order to get high resolution close to the surface, giving 8 computational levels up to 100 m height, while higher up the grid points becomes more and more linearly spaced, and the model top is at the height 10000 m, where the vertical resolution is 760 m.

Note that the height is always given as height above the so called zero-displacement. The magnitude of the zero-displacement is typically about 3/4 of the average canopy height. For example a forest with an average tree height of 20 m, will have a zero-displacement height, which is about 15 m. Thus in this example the model result at for example 72 m height means 72+15=87 m above ground.

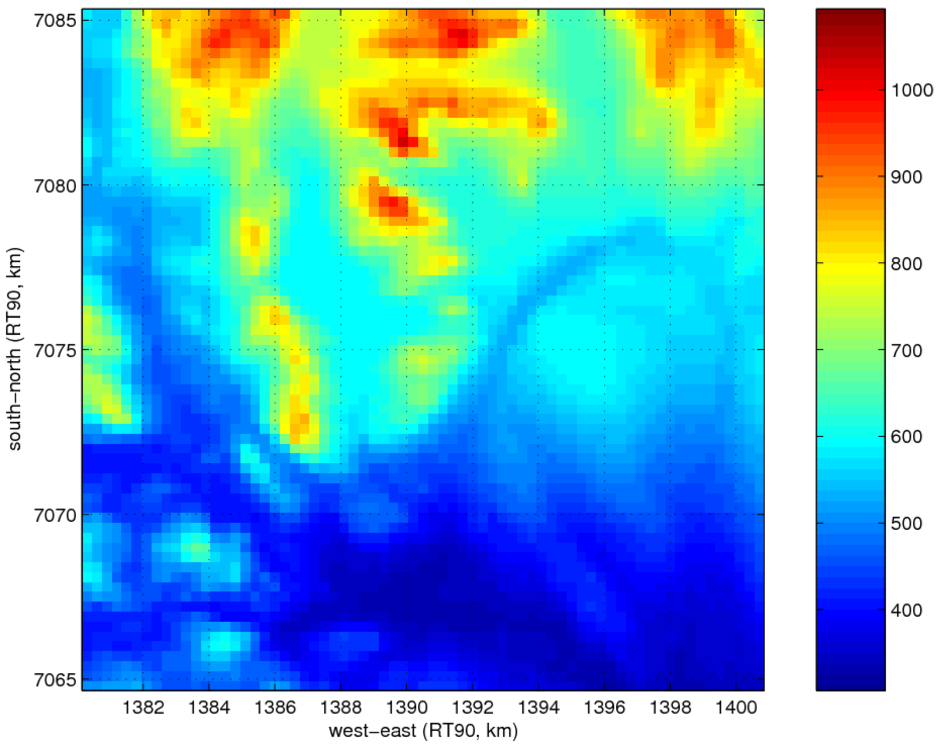

Figure 1: Map showing topography in the model domain covering Storrun as 'seen' by the model with 300 m resolution. Colours give heights in m above sea level.

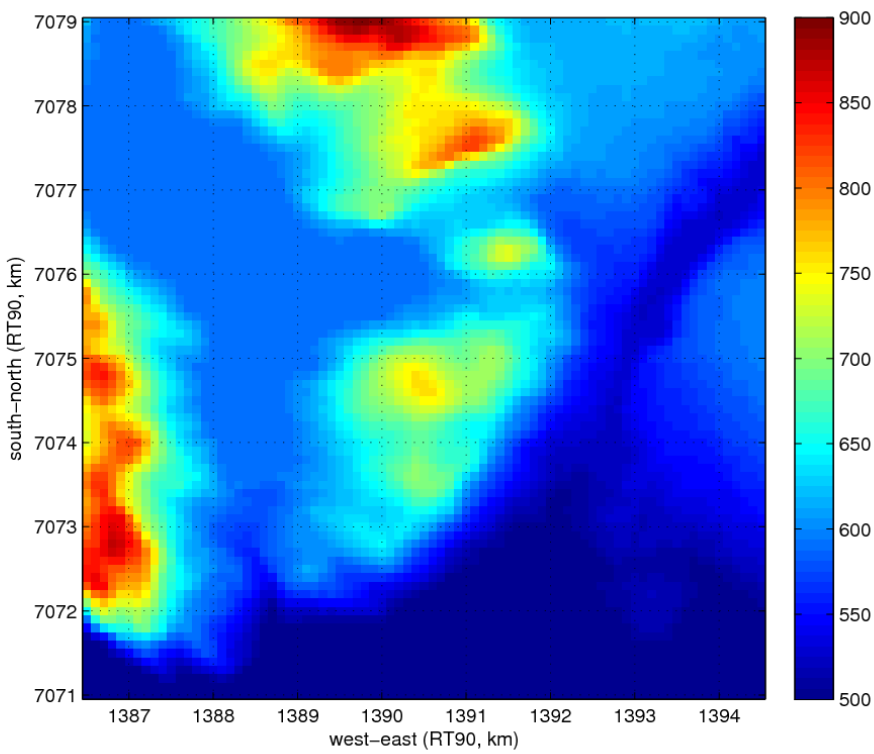

Figure 2: Map showing topography in the model domain covering Storrun as 'seen' by the model with 100 m resolution. Colours give heights in m above sea level.

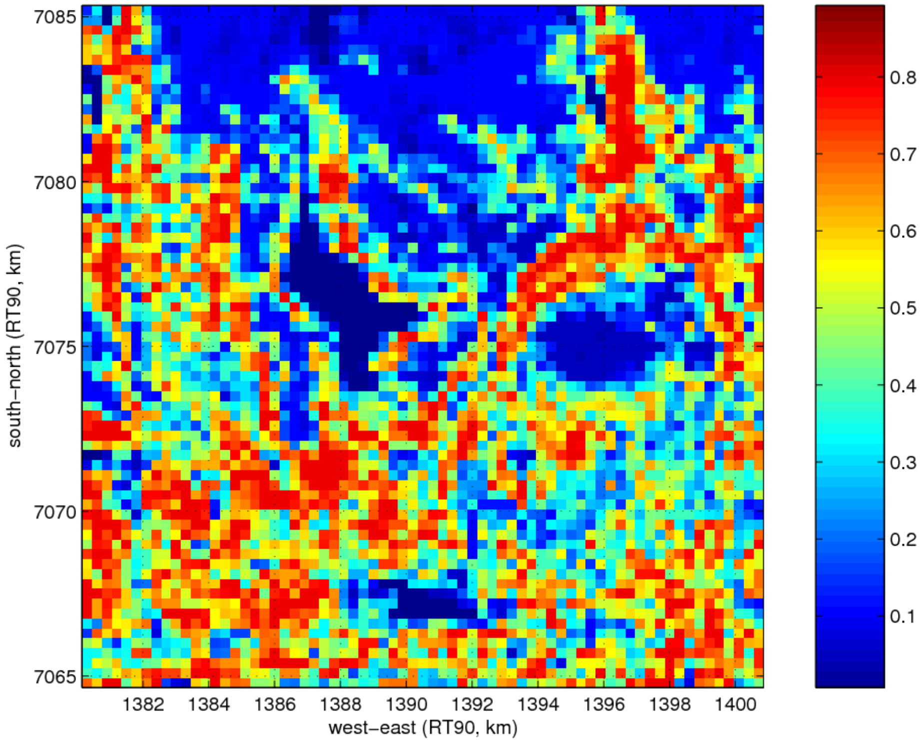

Figure 3: Map showing roughness lengths z_0 (m) in the model domain covering Storrun as 'seen' by the model with 300 m resolution.

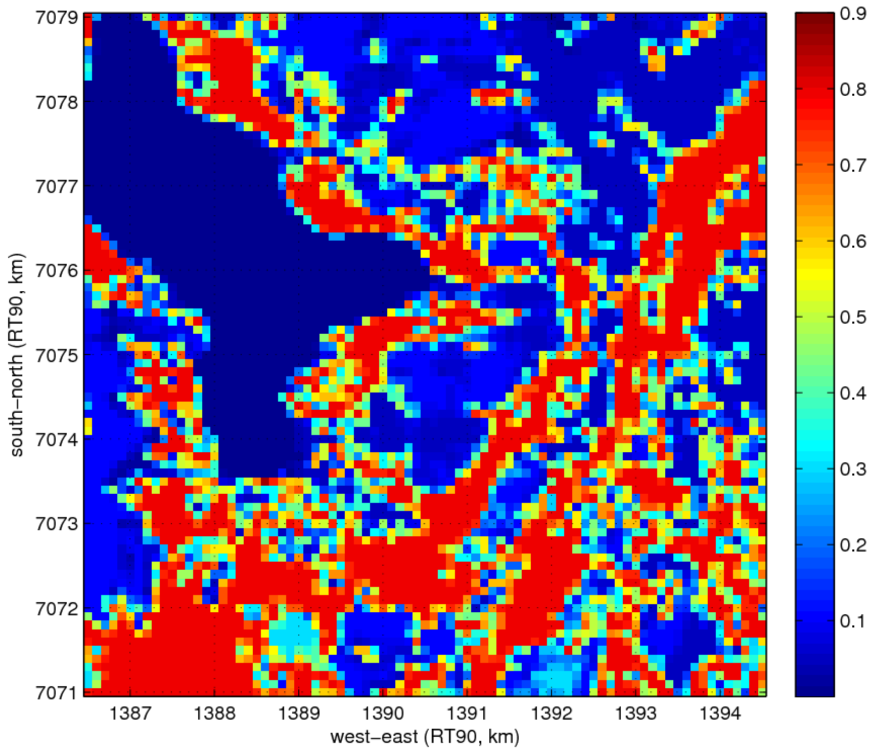

Figure 4: Map showing roughness lengths z_0 (m) in the model domain covering Storrun as 'seen' by the model with 100 m resolution.

4 Mean wind climate estimates

A summation over all model runs made (192 representing 4 seasons, 3 strengths and 16 directions of the geostrophic wind) and hours (each model runs gives an output of 24 hours – a diurnal cycle), gives the climate mean value for each grid point and each height. Statistics of the horizontal air pressure gradient (the geostrophic wind) is used to weight the results into a long-term climatological average. Mean sea level pressure data from observations at Bodö, Härnösand and Haparanda 1900-2000 were used to get the geostrophic wind statistics. The pressure data had previously been checked and corrected for inhomogeneities (Schmith et al. 1997). A correction for the geographical variations of the geostrophic wind has also been made, following the results using NCEP/NCAR reanalysis data (Kalnay et al. 1996).

The annual mean wind speed at 2 heights, 72, and 103 m using both 300 m and 100 m resolution are shown in Figure 5 to Figure 12. The modelled annual average wind speed profiles at the two positions with wind measurements at Storrun are shown in **Figure 13**.

It is important to remember the 1 km resolution used in the model. With this resolution not all details in the terrain will be resolved. Thus the locations of the wind speed iso-lines should not be regarded as accurate to more than within 1 km or so.

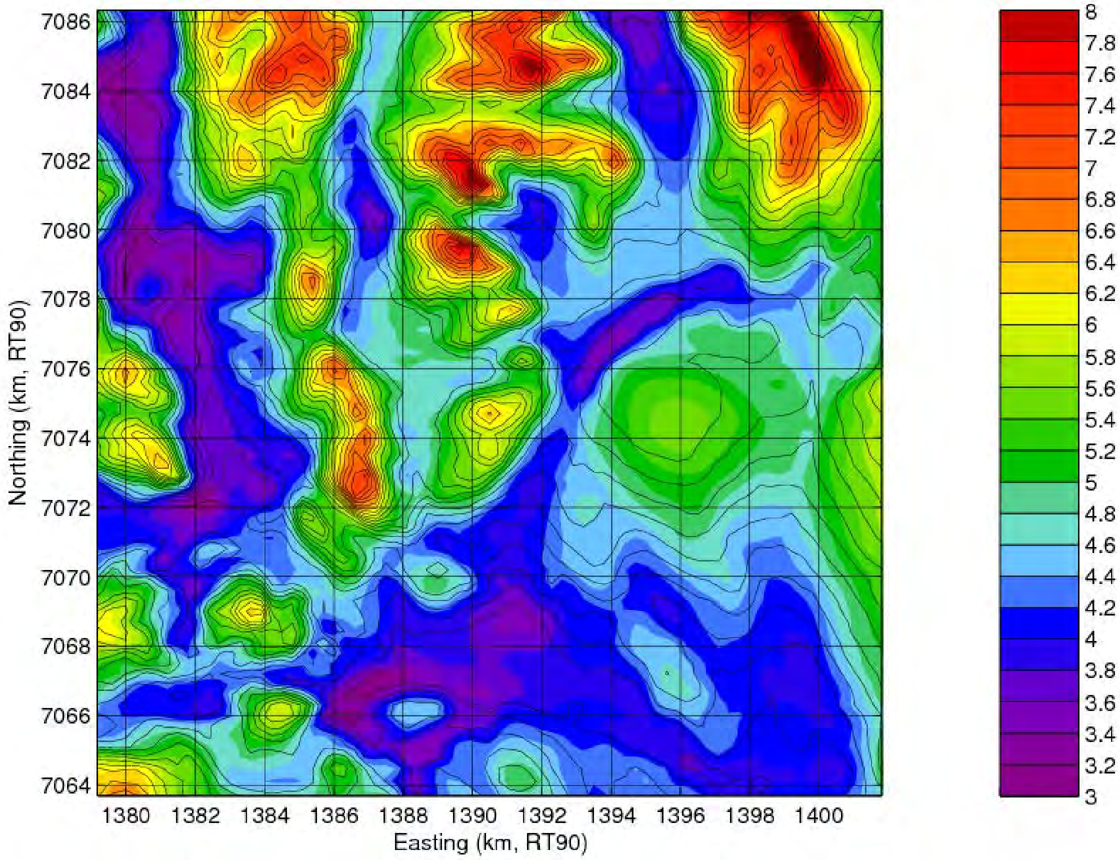

Figure 5: Modelled annual average wind speed at height 72 m above zero-plane displacement, 300 m x 300 m grid resolution.

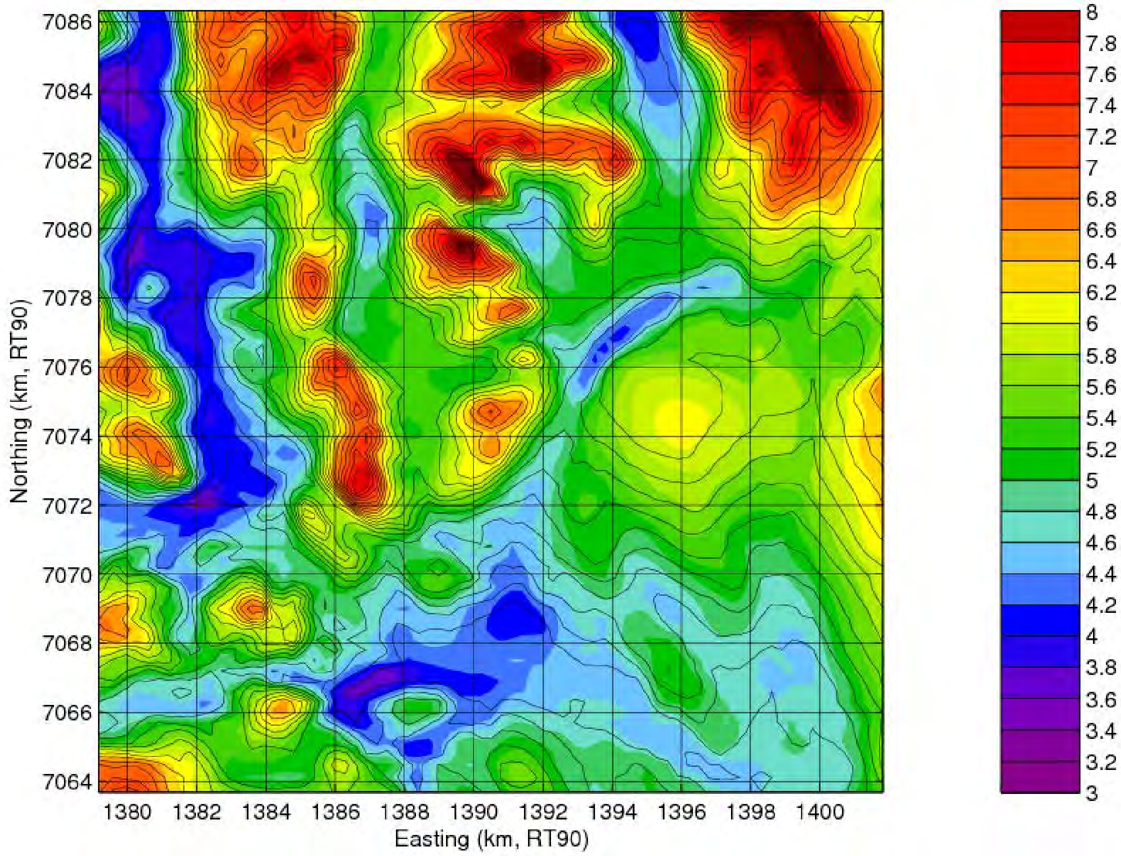

Figure 6: Modelled annual average wind speed at height 103 m above zero-plane displacement, 300 m x 300 m resolution.

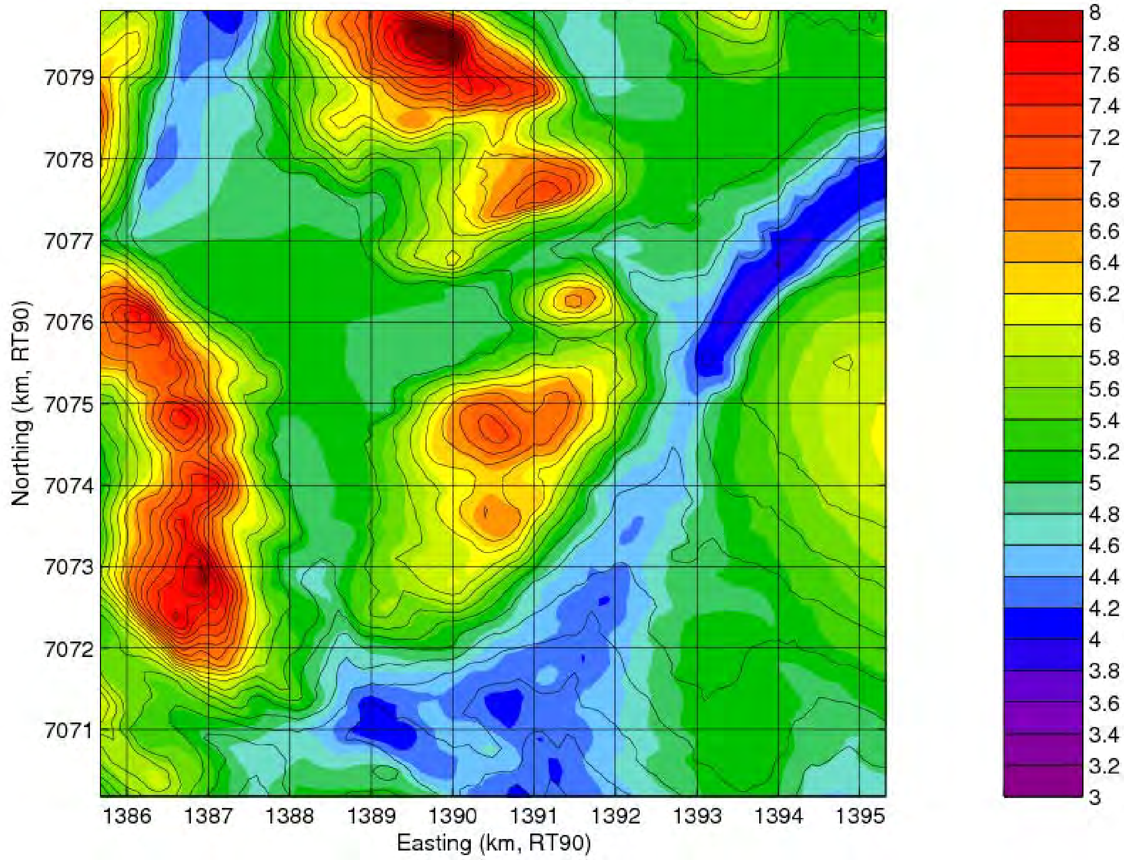

Figure 7: Modelled annual average wind speed at height 72 m above zero-plane displacement, 100 m x 100 m grid resolution.

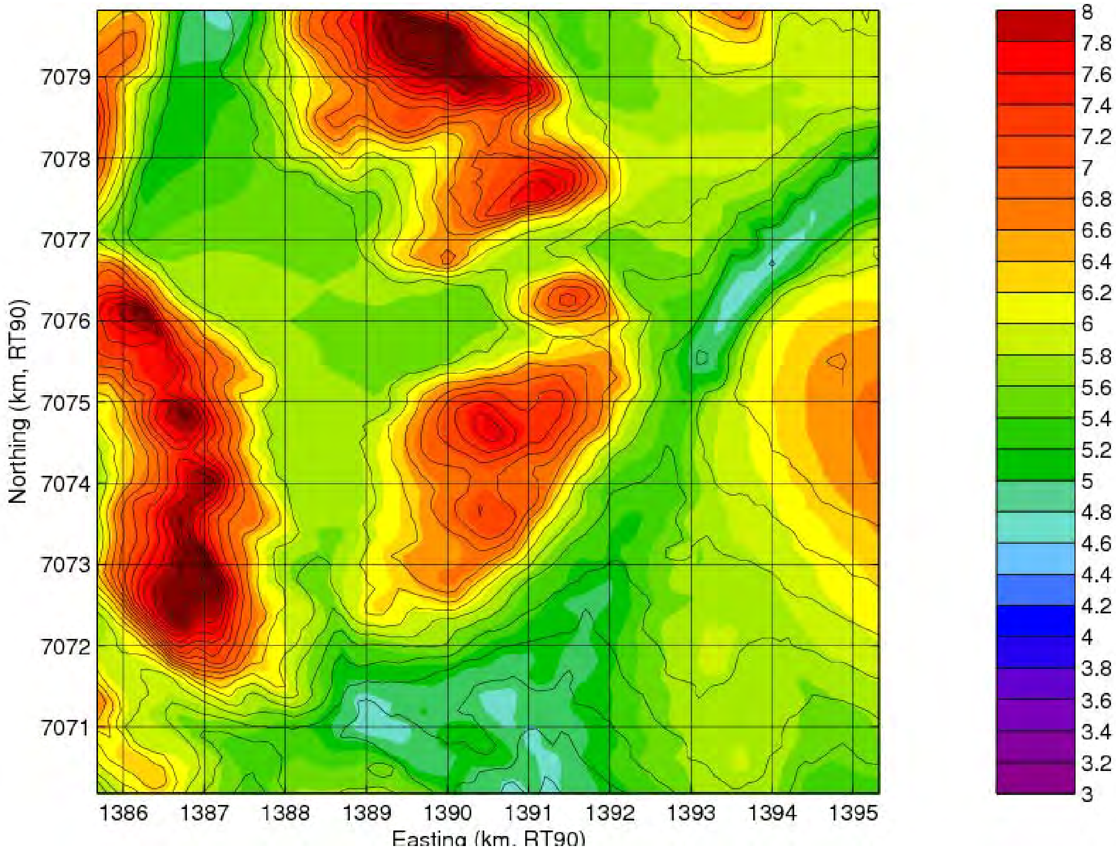

Figure 8: Modelled annual average wind speed at height 103 m above zero-plane displacement, 100 m x 100 m grid resolution.

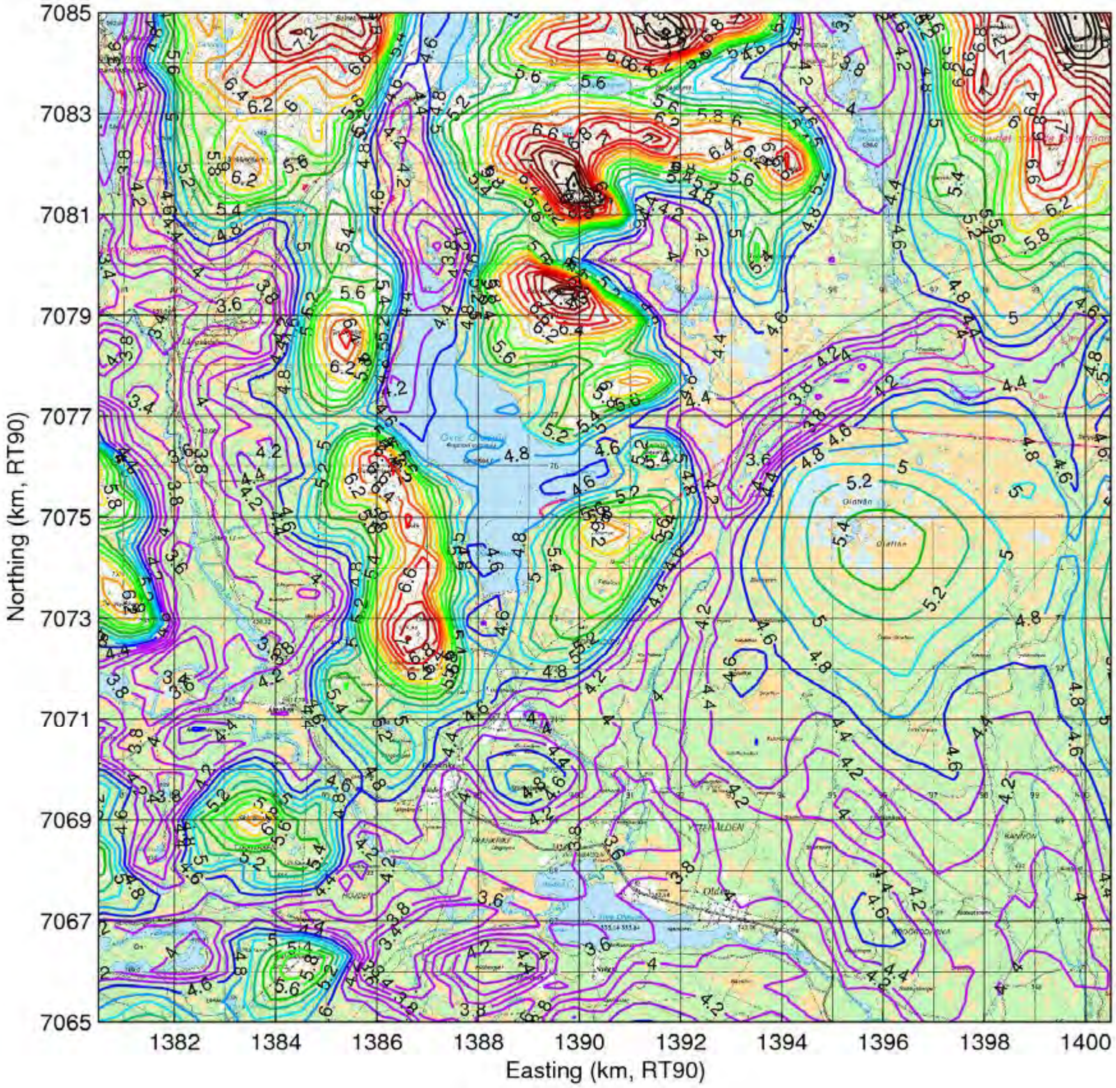

Figure 9: Modelled annual average wind speed at height 72 m above zero-plane displacement, 300 m x 300 m resolution.

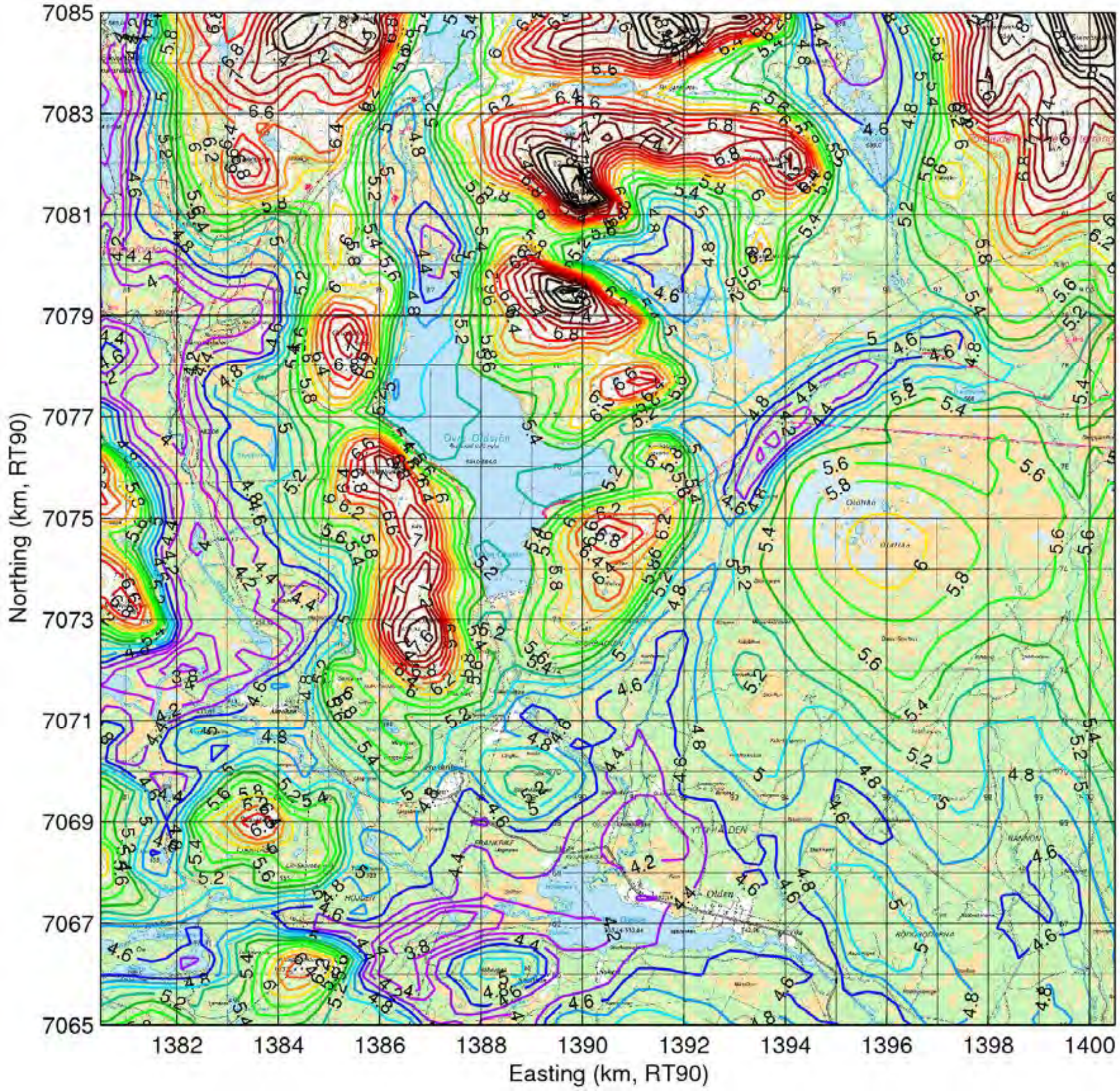

Figure 10: Modelled annual average wind speed at height 103 m above zero-plane displacement, 300 m x 300 m resolution.

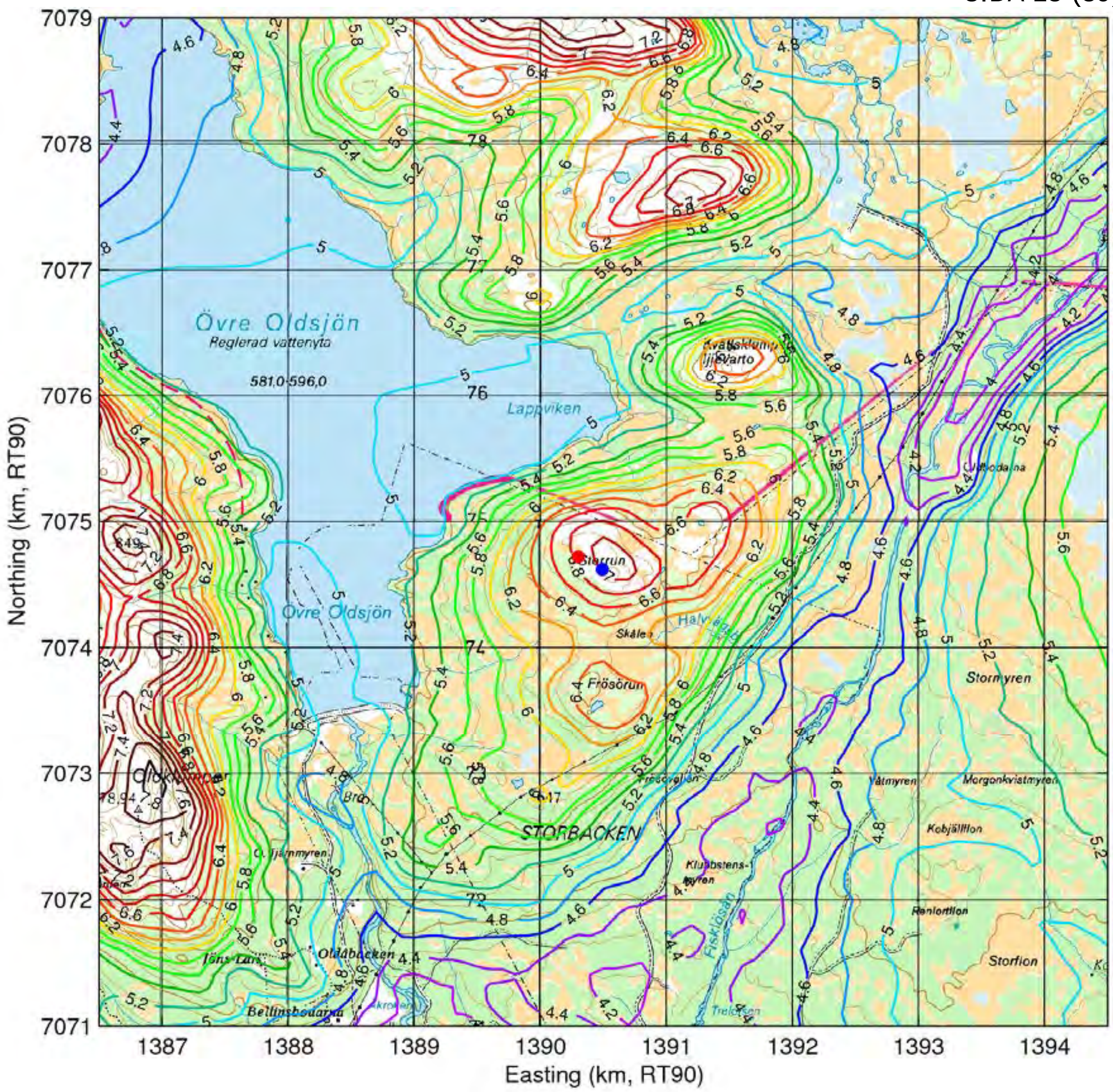

Figure 11: Modelled annual average wind speed at height 72 m above zero-plane displacement, 100 m x 100 m resolution. The two wind measurement sites at Storrun are marked with the red and blue dots.

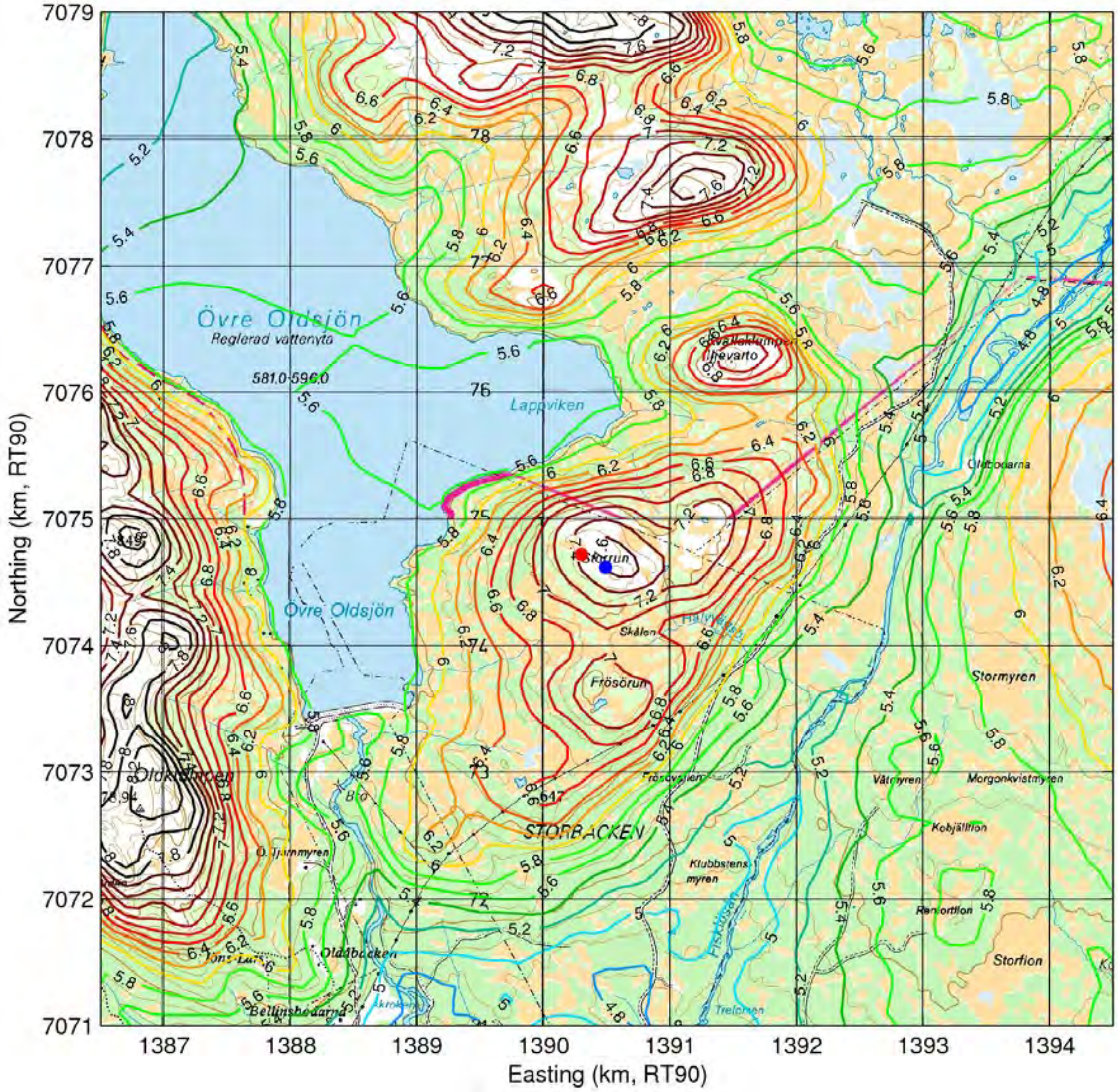

Figure 12: Modelled annual average wind speed at height 103 m above zero-plane displacement, 100 m x 100 m resolution. The two wind measurement sites at Storrun are marked with the red and blue dots.

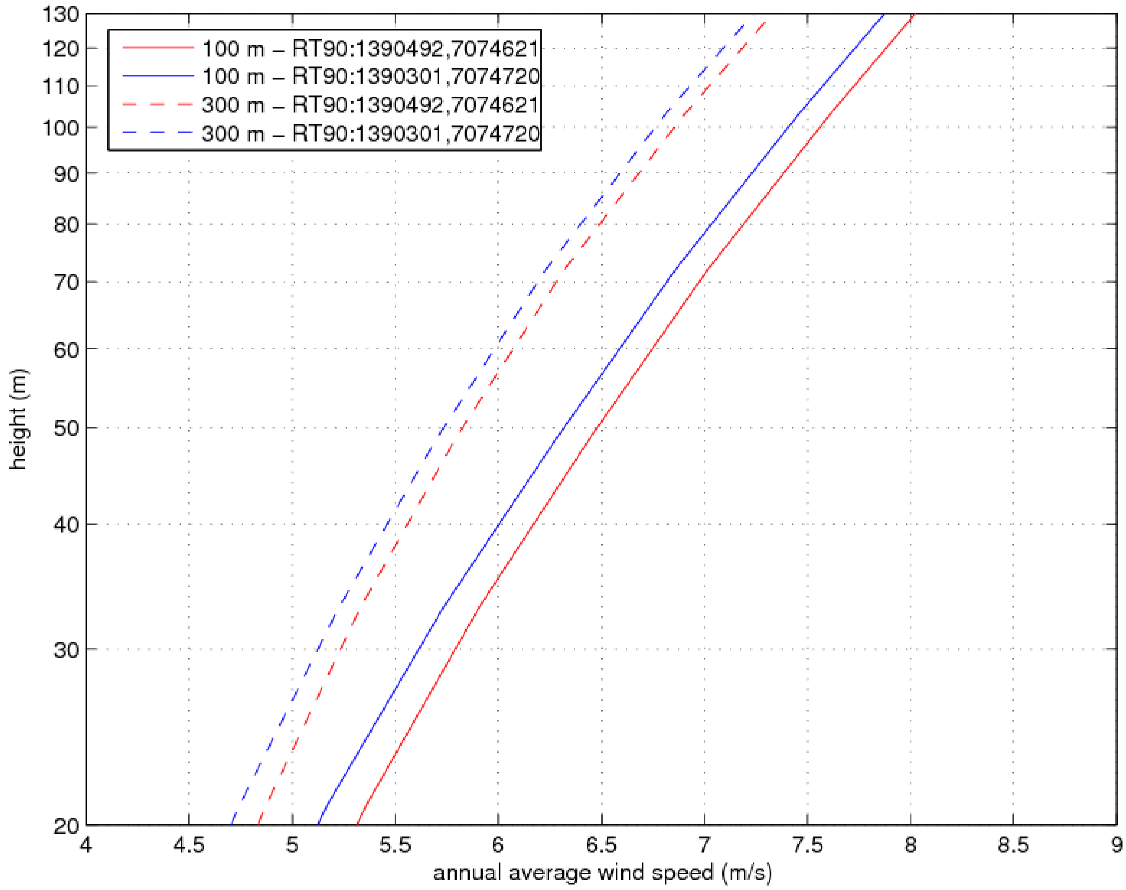

Figure 13: Modelled annual average wind speed profiles at the two positions with wind measurements at Storrun. Model results using 300 m and 100 m resolution.

5 Wind measurements at Storrun

Wind measurements made at two locations and during three periods have been supplied by Dong. Results from an analysis of these data are presented in this section.

5.1 Storrun site 1

The measurement site is located at Site 1, Storrun (RT90:1390301,7074720). The site is shown by the red dot in Figure 11.

The measurements are taken on a 30 m high tower. Wind speed measurements were taken at 1 level, 30 m. A wind vane is used to measure wind direction.

All data have been sampled as 10 min averages, together with turbulence intensity.

5.1.1 RESULTS

Time series of wind speed and wind direction Site 1, Storrun, during the period 14 January 2005 to 7 February 2008 are shown in Figure 14.

The data availability on a monthly basis is plotted in Figure 15, and shows that data is available during 100 % of the time except for a period from January 2006 to October 2007. Some reductions of data due to icing are found for the winter periods. These data were not included in the analysis.

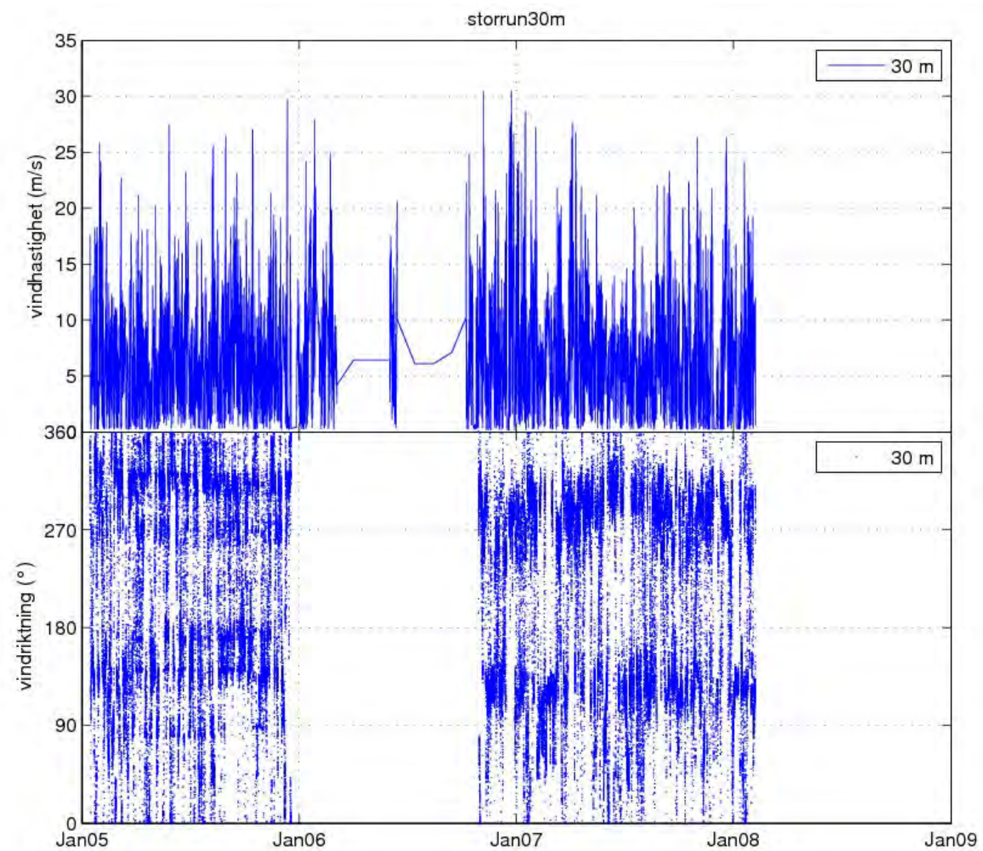

Figure 14: Time series (10 min averages) of, from top to bottom: Wind speed and wind direction. Measurements taken at Site 1, Storrun, 14 January 2005 to 7 February 2008.

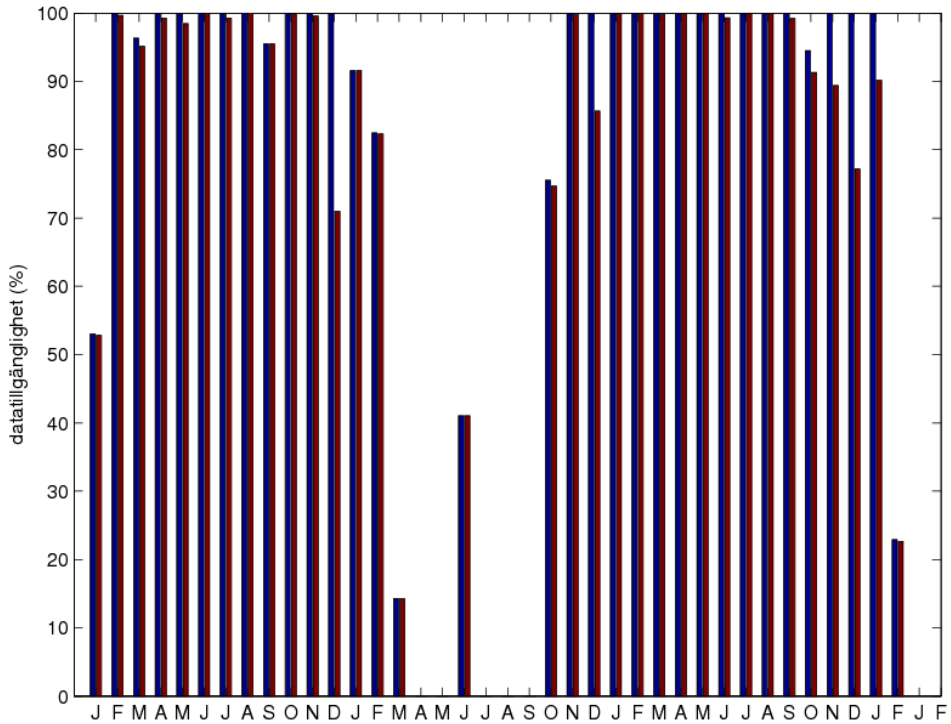

Figure 15: Data availability on a monthly basis for the measurement system at Site 1, Storrun, 14 January 2005 to 7 February 2008. Left hand bars for each month show availability of the logger system while right hand bars show availability after removal of measurements affected by icing or other errors.

The mean wind speed distribution at 30 m height is shown in Figure 16a. The peak is found at about 4-5 m/s, and the observed mean wind speed for the observation period, 14 January 2005 to 7 February 2008, is 6.82 m/s. The Weibull distribution,

$$f(U) = \frac{c}{A}\left(\frac{U}{A}\right)^{(c-1)} \cdot e^{-\left(\frac{U}{A}\right)^{c}}, \quad (1)$$

which has been adapted to the observations, is given by the full line in Figure 16a. The corresponding scale parameter, A, was estimated to 7.63 m/s and the shape parameter, c, to 1.62.

The wind direction distribution is given in Figure 16b. The peak in the distribution is found for winds from westnorthwest but winds from southeast are also quite common.

The daily variation of mean wind speed is shown in Figure 17. The daily amplitude is as a mean about 0.6 m/s at 30 m. The maximum winds are found during the afternoon and a minimum in the morning.

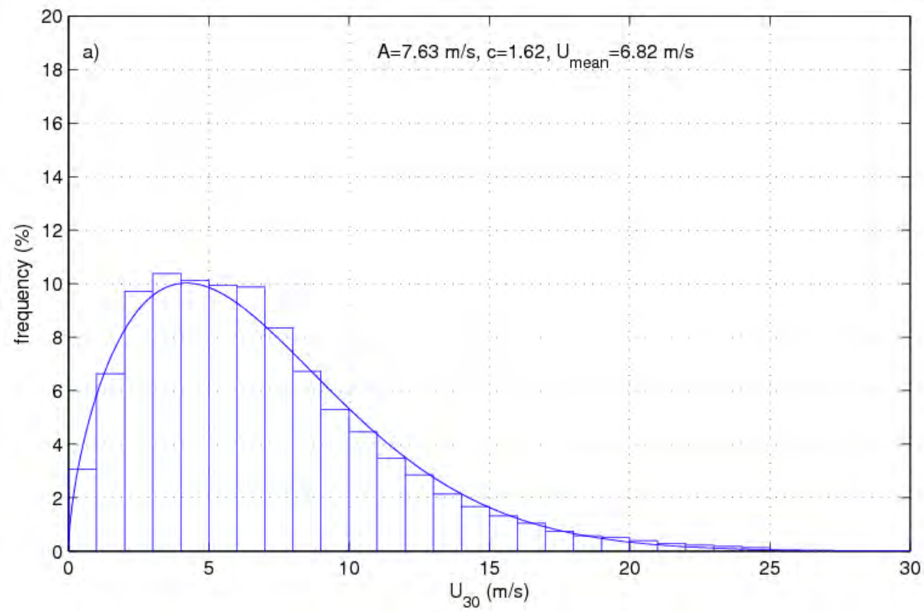

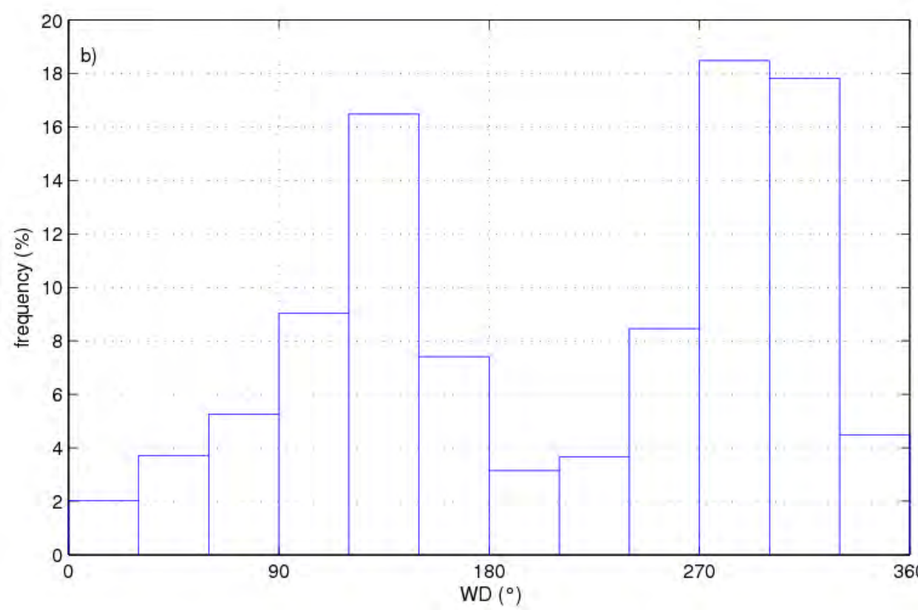

Figure 16. a) Observed (bars) distribution of mean wind speed at Site 1, Storrun, 104 m height, for the period 14 January 2005 to 7 February 2008. The curve shows the Weibull distribution adapted to the observations. b) Observed distribution of wind direction at Site 1, Storrun.

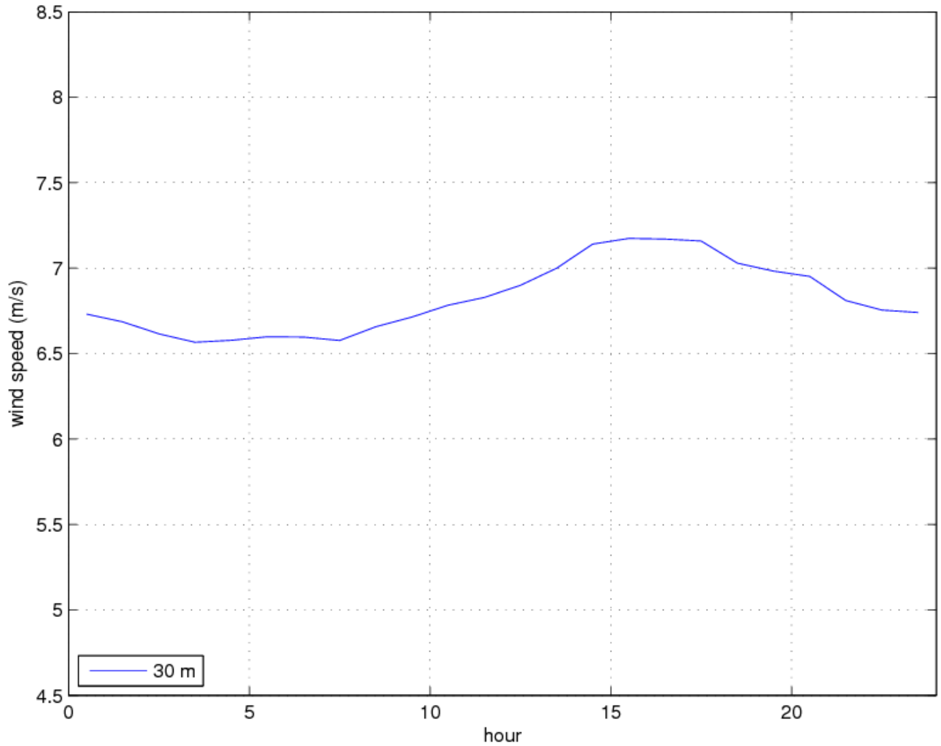

Figure 17: Hourly average wind speed at Site 1, Storrun, for the period 14 January 2005 to 7 February 2008.

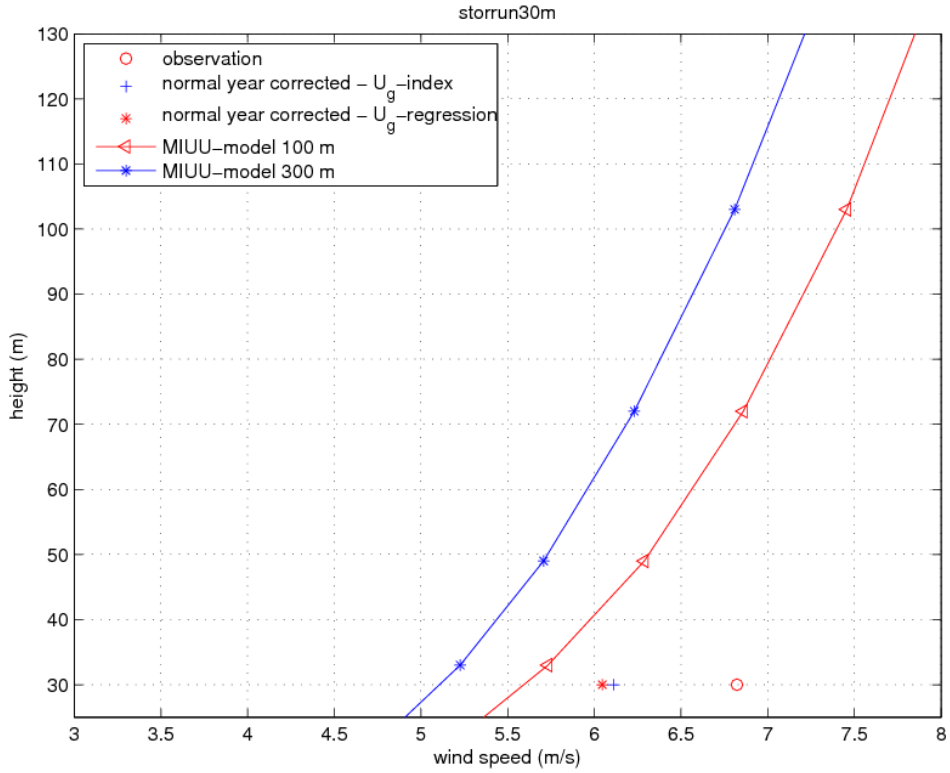

Figure 18: Observed average wind speed at Site 1, Storrun, during period 14 January 2005 to 7 February 2008. The full line gives the corresponding modelled profiles. Also the long-time corrected wind speed is shown.

The observed average wind speed profile at Site 1, Storrun, is shown in Figure 18. For the period 14 January 2005 to 7 February 2008 the average wind speed is 6.8 m/s at 30 m.

Also included in Figure 18 is long-time corrected wind arrived at using the geostrophic winds at the site during the measurements period. According to these data the measurements period should have had an average wind about 12 % above the long-time average giving the long-time corrected average wind speed 6.1 m/s.

A correction based upon simultaneous data every six hours for the geostrophic wind speed and measured wind speed gives an average 13 % below the long-time average, and resulted in the long-time corrected average wind speed 6.0 m/s at 30 m height. The relation is shown in Figure 19.

An uncertainty analysis made using long-time measurements at Näsudden on Gotland show that after 30 months observation time the uncertainty could be expected to be about ±0.3 m/s with a 95 % confidence limit (Nilsson and Bergström, 2009).

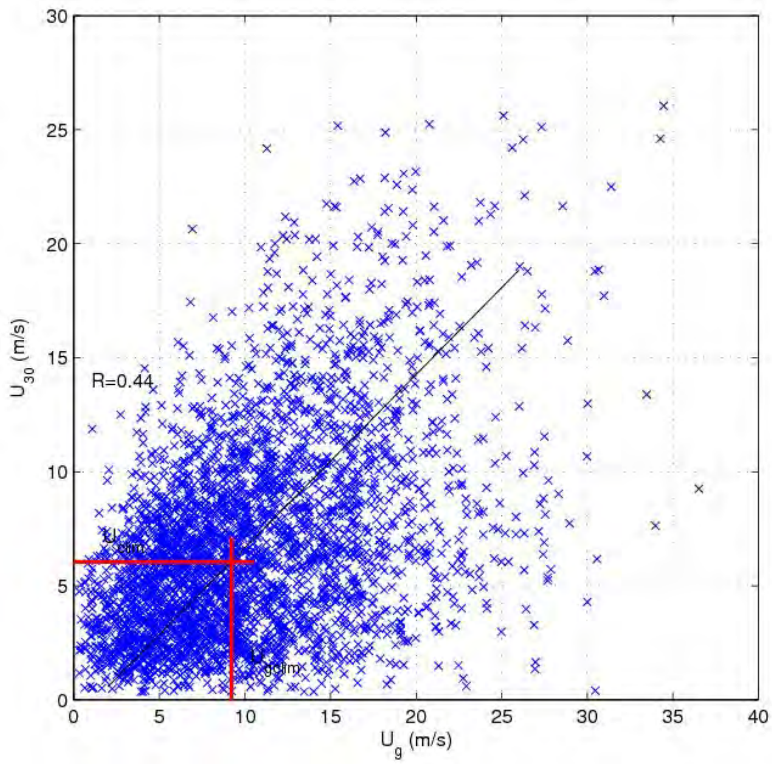

Figure 19: Relation between simultaneous observations of geostrophic wind speed U_g and observed wind speed at 104 m height. Data from the period 14 January 2005 to 7 February 2008 with observations every 6 hour. The correlation coefficient is 0.44. U_{gclim} is the average geostrophic wind speed, 9.2 m/s, and reading off the regression line gives the expected long-time average wind speed at 30 m height, U_{clim}=6.0 m/s.

5.2 Storrun site 2 Vaisala

The measurement site is located at Site 2, Storrun (RT90:1390492,7074621). The site is shown by the blue dot in Figure 11.

The measurements are taken on a 50 m high tower. Wind speed measurements were taken at 2 levels, 30 m and 50 m. A wind vane is used to measure wind direction at 50 m. Also temperature was measured. The instrumentation consists of heated Vaisala anemometers and wind vane.

All data have been sampled as 10 min averages, together with turbulence intensity.

5.2.1 RESULTS

Time series of wind speed, wind direction and temperature, Site 2, Storrun, during the period 20 January 2007 to 7 February 2008 are shown in Figure 20.

The data availability on a monthly basis is plotted in Figure 21, and shows that data is available during 100 % of the time. Some smaller reductions of data due to icing are found for the winter periods. These data were not included in the analysis.

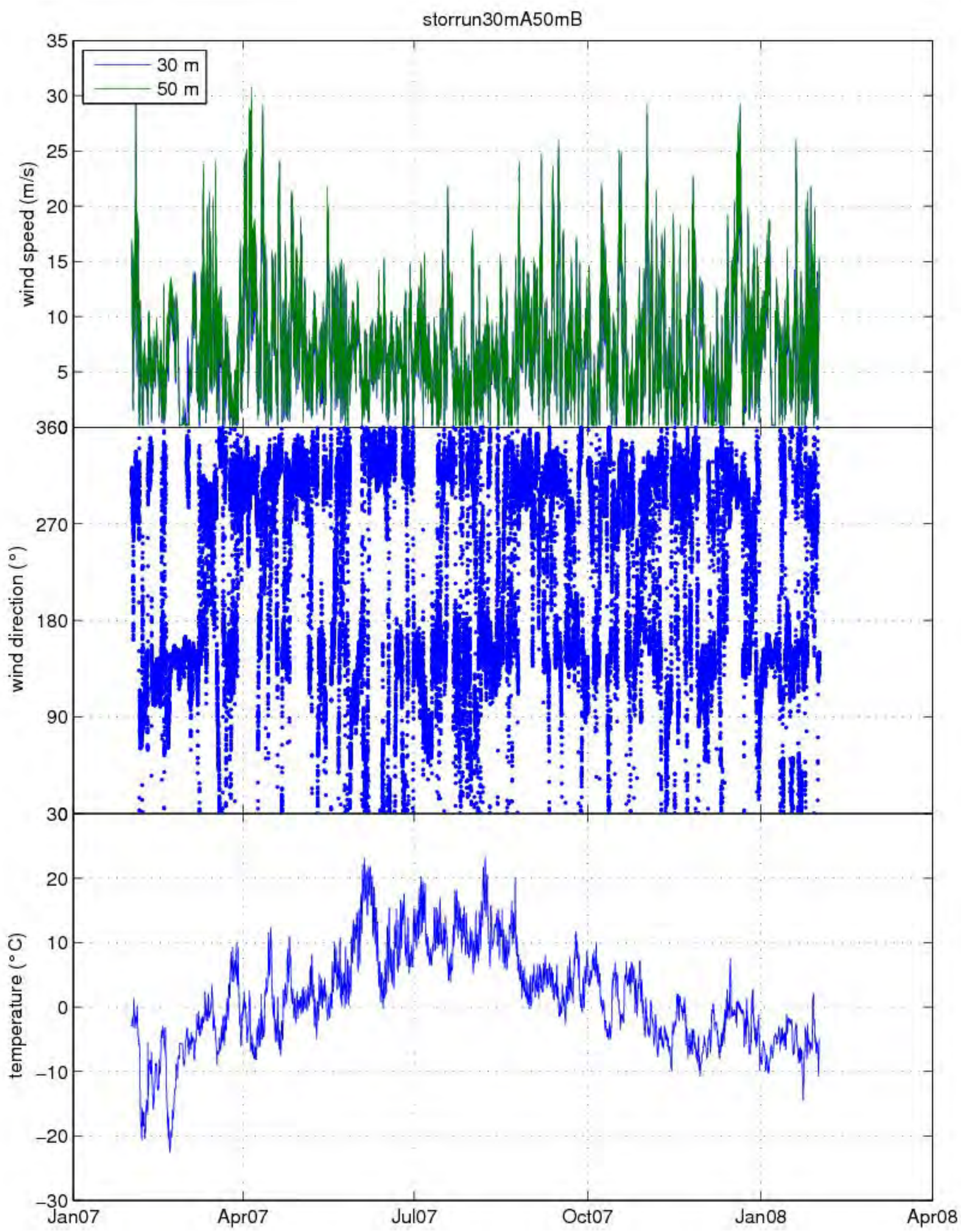

Figure 20: Time series (10 min averages) of, from top to bottom: Wind speed and wind direction. Measurements taken at Site 2, Storrun, 20 January 2007 to 7 February 2008.

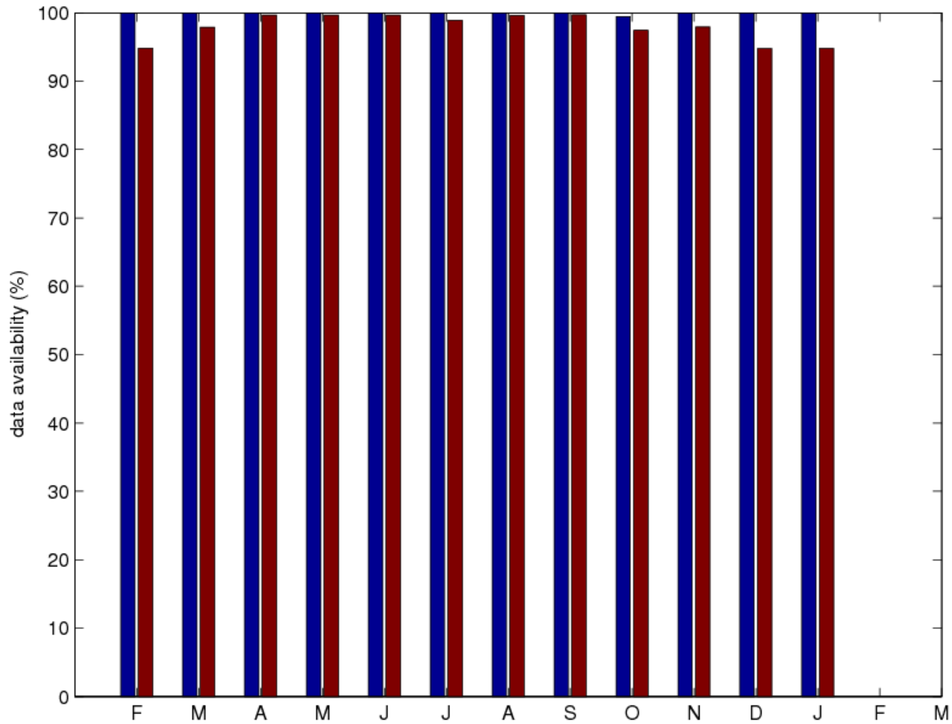

Figure 21: Data availability on a monthly basis for the measurement system at Site 2, Storrun, 20 January 2007 to 7 February 2008. Left hand bars for each month show availability of the logger system while right hand bars show availability after removal of measurements affected by icing or other errors.

The mean wind speed distribution at 50 m height is shown in Figure 22a. The peak is found at about 4-5 m/s, and the observed mean wind speed for the observation period, 20 January 2007 to 7 February 2008, is 7.35 m/s. The Weibull distribution,

$$f(U) = \frac{c}{A}\left(\frac{U}{A}\right)^{(c-1)} \cdot e^{-\left(\frac{U}{A}\right)^{c}},$$

which has been adapted to the observations, is given by the full line in Figure 16a. The corresponding scale parameter, *A*, was estimated to 8.16 m/s and the shape parameter, *c*, to 1.58.

The wind direction distribution is given in Figure 22b. The peak in the distribution is found for winds from northwest but winds from southeast are also quite common.

The daily variation of mean wind speed is shown in Figure 23. The daily amplitude is as a mean about 0.9 m/s both at 30 m and 50 m. The maximum winds are found during the afternoon and a minimum in the morning.

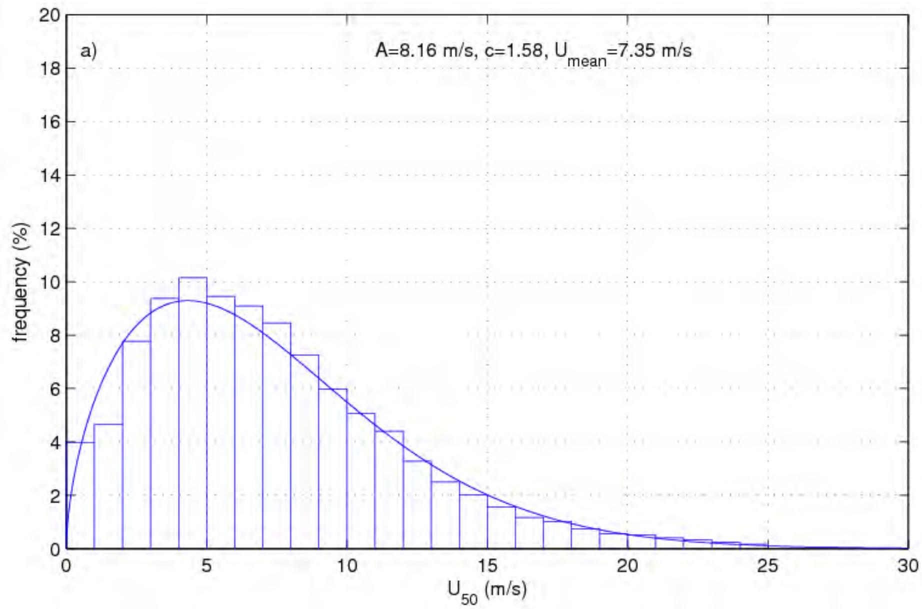

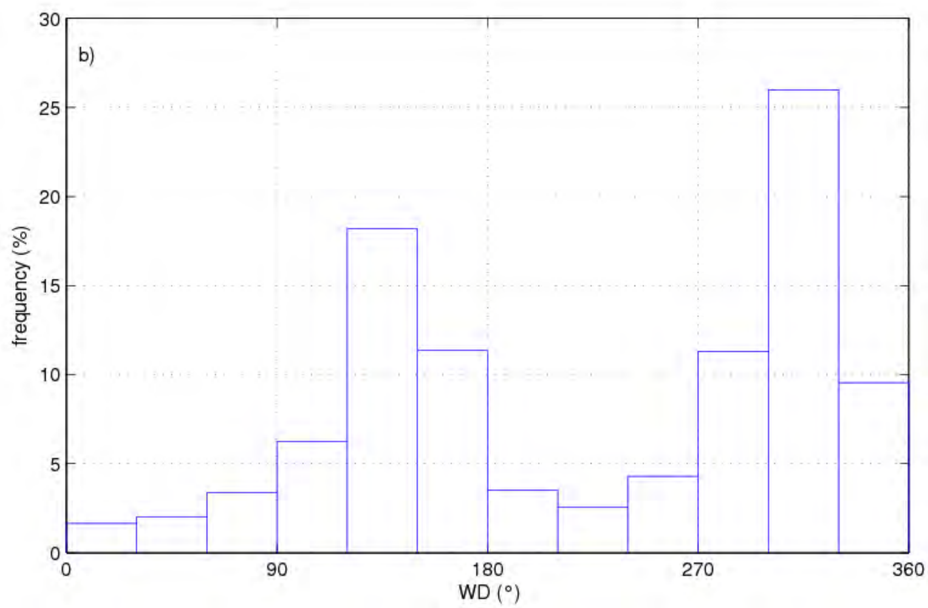

Figure 22. a) Observed (bars) distribution of mean wind speed at Site 2, Storrun, 104 m height, for the period 20 January 2007 to 7 February 2008. The curve shows the Weibull distribution adapted to the observations. b) Observed distribution of wind direction at Site 2, Storrun.

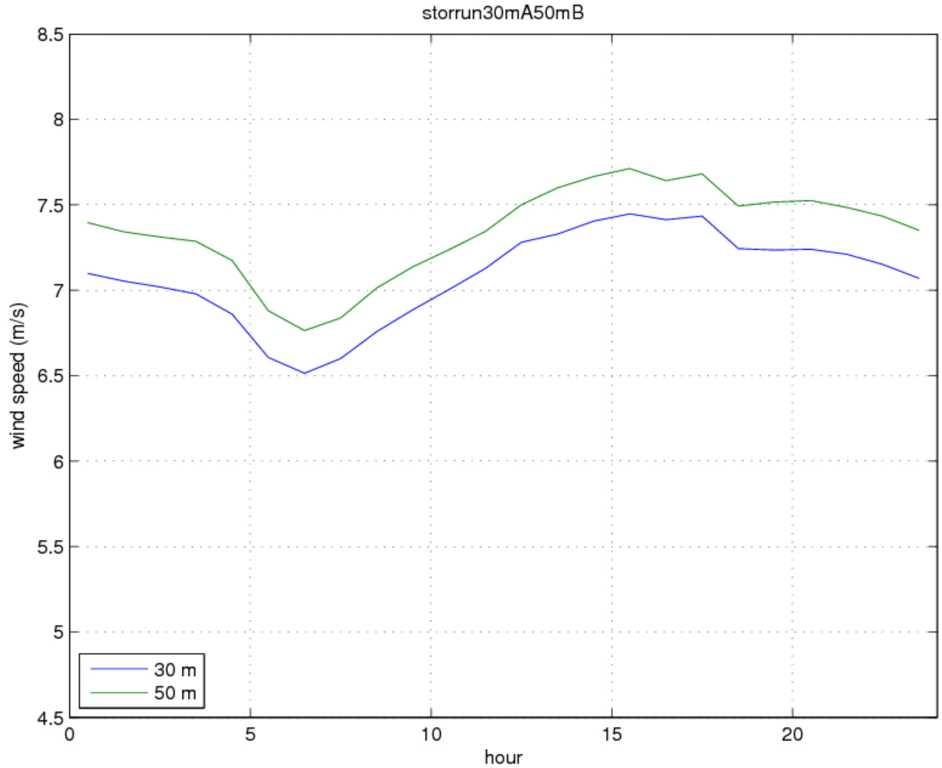

Figure 23: Hourly average wind speed at Site 2, Storrun, for the period 20 January 2007 to 7 February 2008.

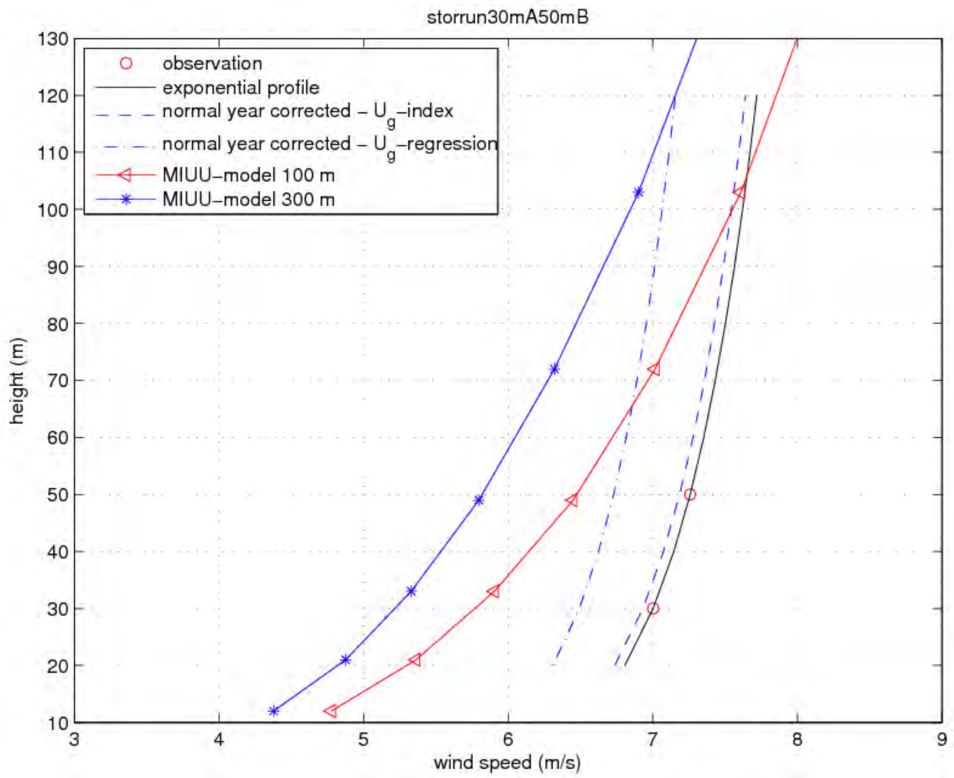

Figure 24: Observed average wind speed profile at Site 2, Storrun, during the period 20 January 2007 to 7 February 2008. The full line gives the corresponding modelled profiles. Also the long-time corrected wind speed profiles according to two method are shown.

The observed average wind speed profile at Site 2, Storrun, is shown in Figure 24. For the period 20 January 2007 to 7 February 2008 the average wind speed increases from 7.0 m/s at 30 m to 7.5 m/s at 50 m. Assuming that the vertical wind profile could be described by an exponential profile given by

$$\frac{U(z_2)}{U(z_1)} = \left(\frac{z_2}{z_1}\right)^{\alpha} \qquad (2)$$

where U=wind speed and z=height, the value of the exponent α is determined to 0.070. The exponential profile is also shown in Figure 24.

Also included in Figure 24 is long-time corrected profiles arrived at using the geostrophic winds at the site during the measurements period. According to these data the measurements period should have had an average wind about 1 % above the average for the period 1979-2008. The correction is then based on monthly averages during the measurement period and a total average estimated based on long time corrected monthly averages. The long-time corrected annual average wind speed at 50 m based on this u_g-index is 7.2 m/s.

A correction based upon simultaneous data every six hours for the geostrophic wind speed and measured wind speed gives an average 8 % above the long-time average, and resulted in the long-time corrected average wind speed 6.8 m/s at 50 m height. The relation is shown in Figure 25.

An uncertainty analysis made using long-time measurements at Näsudden on Gotland show that after 12 months observation time the uncertainty could be expected to be about ±0.4 m/s with a 95 % confidence limit (Nilsson and Bergström, 2009).

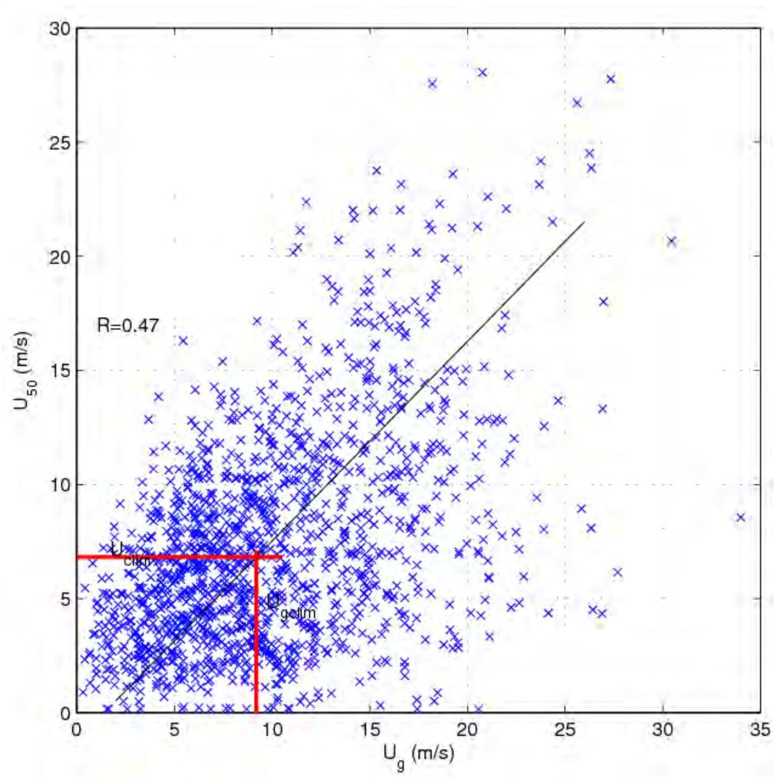

Figure 25: Relation between simultaneous observations of geostrophic wind speed U_g and observed wind speed at 104 m height. Data from the period 20 January 2007 to 7 February 2008 with observations every 6 hour. The correlation coefficient is 0.47. U_{gclim} is the average geostrophic wind speed, 9.2 m/s, and reading off the regression line gives the expected long-time average wind speed at 50 m height, U_{clim}=6.8 m/s.

5.3 Storrun site 2 NRG

The measurement site is located at Site 2, Storrun (RT90:1390492,7074621). The site is shown by the blue dot in Figure 11.

The measurements are taken on a 50 m high tower. Wind speed measurements were taken at 2 levels, 30 m and 50 m. A wind vane is used to measure wind direction at 50 m. The instrumentation consists of unheated NRG anemometers and wind vane.

All data have been sampled as 10 min averages, together with turbulence intensity.

5.3.1 RESULTS

Time series of wind speed, wind direction and temperature, Site 2, Storrun, during the period 29 April 2006 to 27 December 2007 are shown in Figure 20.

The data availability on a monthly basis is plotted in Figure 21, and shows that data is available during 100 % of the time except for the winter period. Some further reductions of data due to icing are found for the winter periods. These data were not included in the analysis.

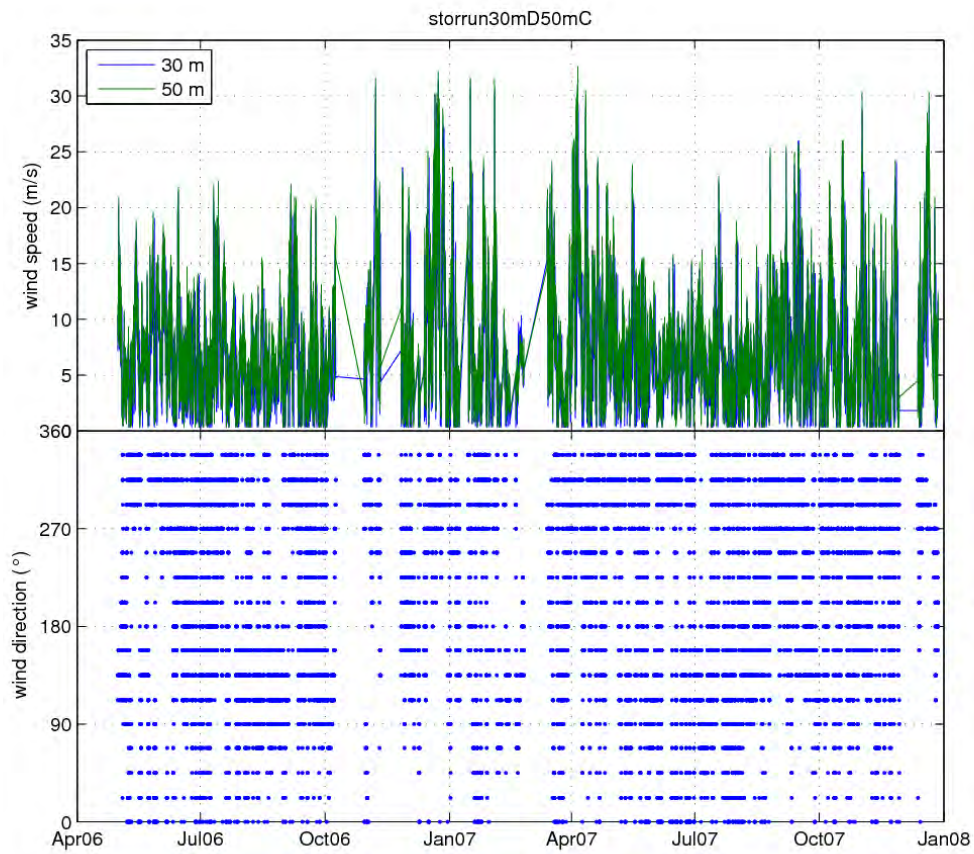

Figure 26: Time series (10 min averages) of, from top to bottom: Wind speed and wind direction. Measurements taken at Site 2, Storrun, 29 April 2006 to 27 December 2007.

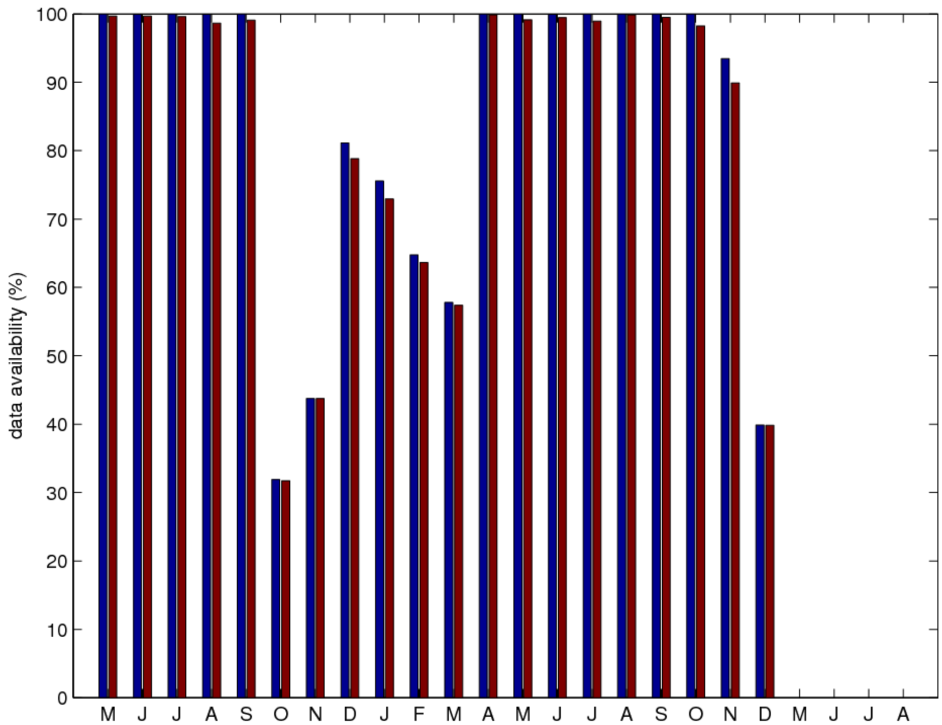

Figure 27: Data availability on a monthly basis for the measurement system at Site 2, Storrun, 29 April 2006 to 27 December 2007. Left hand bars for each month show availability of the logger system while right hand bars show availability after removal of measurements affected by icing or other errors.

The mean wind speed distribution at 50 m height is shown in Figure 22a. The peak is found at about 4-5 m/s, and the observed mean wind speed for the observation period, 29 April 2006 to 27 December 2007, is 7.52 m/s. The Weibull distribution,

$$f(U) = \frac{c}{A}\left(\frac{U}{A}\right)^{(c-1)} \cdot e^{-\left(\frac{U}{A}\right)^{c}},$$

which has been adapted to the observations, is given by the full line in Figure 16a. The corresponding scale parameter, *A*, was estimated to 8.40 m/s and the shape parameter, *c*, to 1.58.

The wind direction distribution is given in Figure 22b. The peak in the distribution is found for winds from westnorthwest but winds from southeast are also quite common.

The daily variation of mean wind speed is shown in Figure 23. The daily amplitude is as a mean about 1.0 m/s both at 30 m and 50 m. The maximum winds are found during the afternoon and a minimum in the morning, but with an unexpected time-lag between the two levels. As no details about the measurement were given, it was not possible to check for possible errors in logging time.

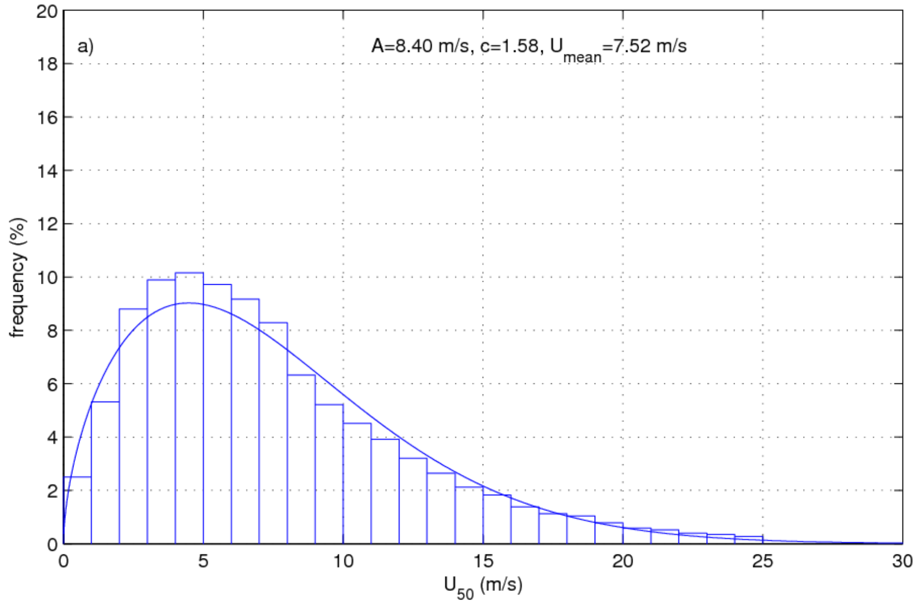

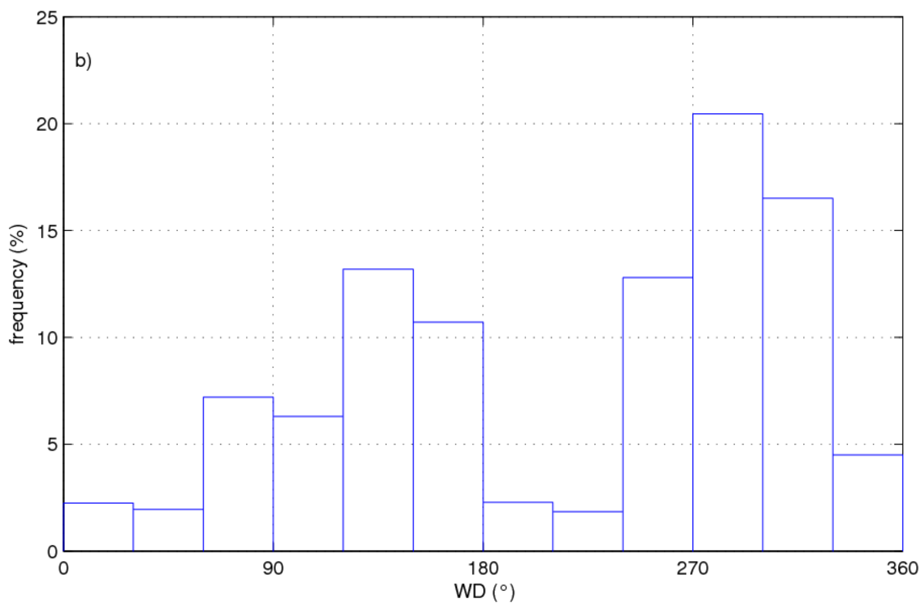

Figure 28. a) Observed (bars) distribution of mean wind speed at Site 2, Storrun, 104 m height, for the period 29 April 2006 to 27 December 2007. The curve shows the Weibull distribution adapted to the observations. b) Observed distribution of wind direction at Site 2, Storrun.

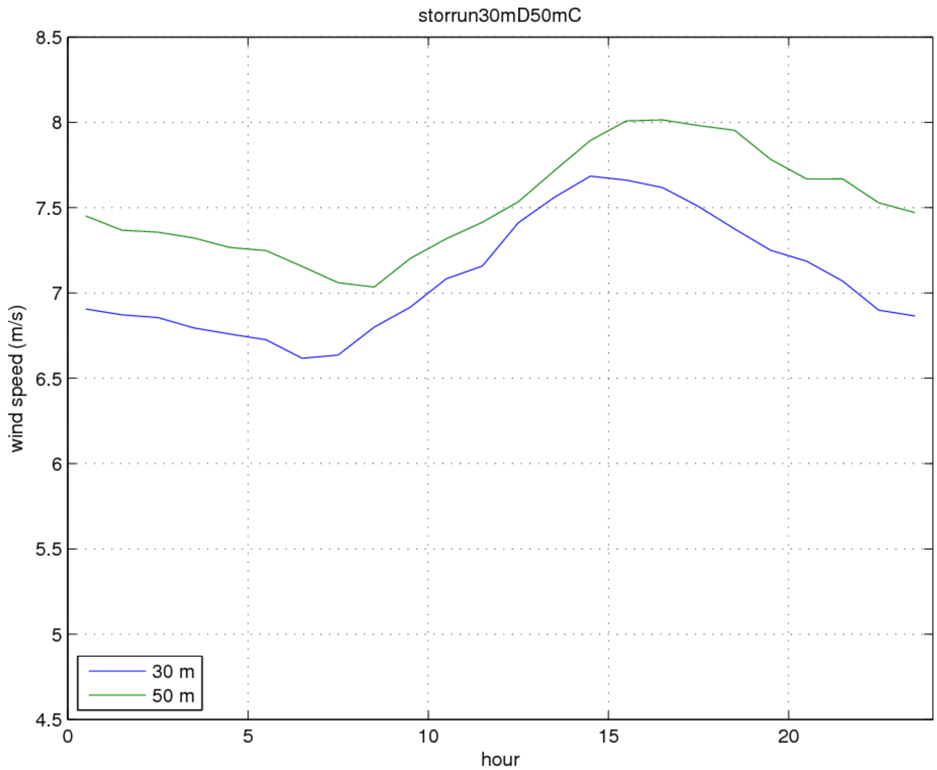

Figure 29: Hourly average wind speed at Site 2, Storrun, for the period 29 April 2006 to 27 December 2007.

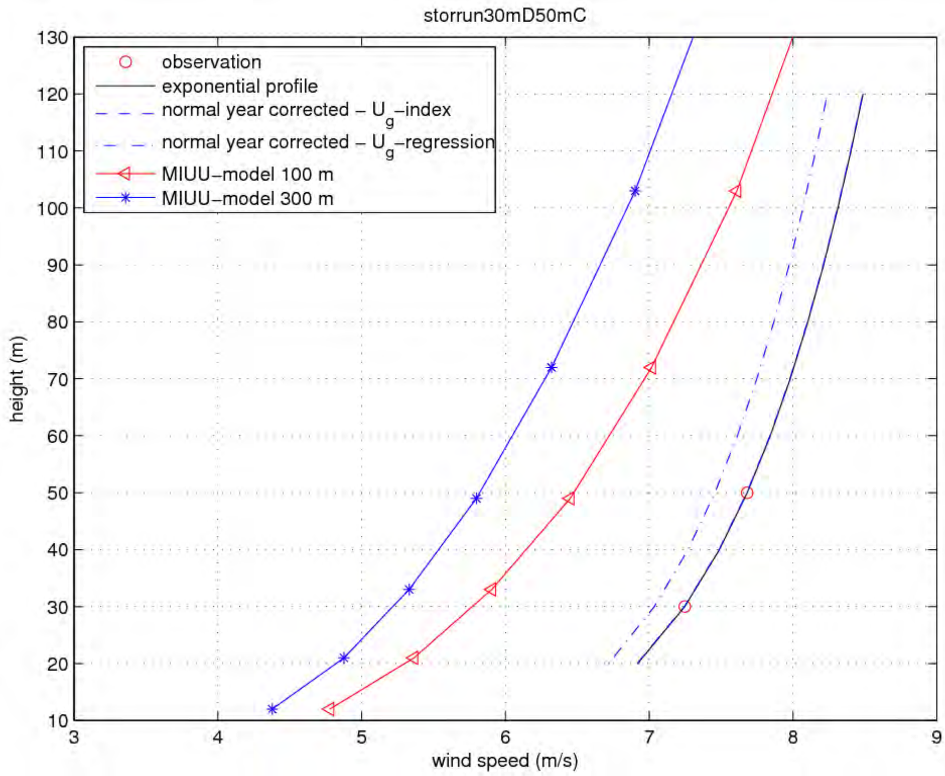

Figure 30: Observed average wind speed profile at Site 2, Storrun, during the period 29 April 2006 to 27 December 2007. The full line gives the corresponding modelled profiles. Also the long-time corrected wind speed profiles according to two method are shown.

The observed average wind speed profile at Site 2, Storrun, is shown in Figure 24. For the period 29 April 2006 to 27 December 2007 the average wind speed increases from 7.2 m/s at 30 m to 7.7 m/s at 50 m. Assuming that the vertical wind profile could be described by an exponential profile given by

$$\frac{U(z_2)}{U(z_1)} = \left(\frac{z_2}{z_1}\right)^{\alpha} \qquad (2)$$

where U=wind speed and z=height, the value of the exponent α is determined to 0.114. The exponential profile is also shown in Figure 24.

Also included in Figure 24 is long-time corrected profiles arrived at using the geostrophic winds at the site during the measurements period. According to these data the measurements period should have had an average wind about the average for the period 1979-2008. The correction is then based on monthly averages during the measurement period and a total average estimated based on long time corrected monthly averages. The long-time corrected annual average wind speed at 50 m based on this u_g-index is 7.7 m/s.

A correction based upon simultaneous data every six hours for the geostrophic wind speed and measured wind speed gives an average 3 % above the long-time average, and resulted in the long-time corrected average wind speed 7.4 m/s at 50 m height. The relation is shown in Figure 25.

An uncertainty analysis made using long-time measurements at Näsudden on Gotland show that after 20 months observation time the uncertainty could be expected to be about ±0.3 m/s with a 95 % confidence limit (Nilsson and Bergström, 2009).

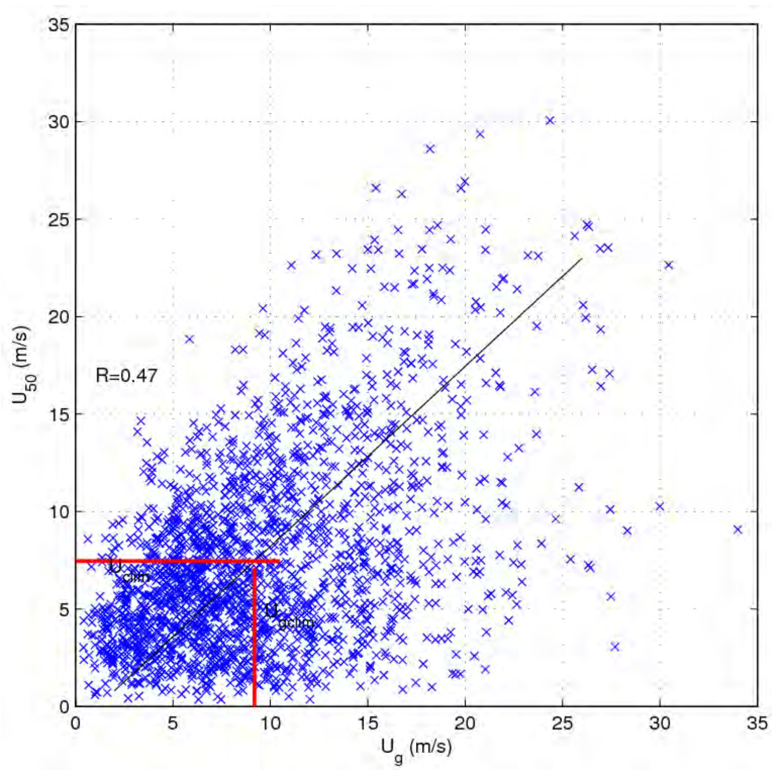

Figure 31: Relation between simultaneous observations of geostrophic wind speed U_g and observed wind speed at 104 m height. Data from the period 29 April 2006 to 27 December 2007 with observations every 6 hour. The correlation coefficient is 0.47. U_{gclim} is the average geostrophic wind speed, 9.2 m/s, and reading off the regression line gives the expected long-time average wind speed at 50 m height, U_{clim}=7.4 m/s.

6. Comparing model results and observations

The analyses made from the available measurement data show quite large differences between the different data sets and different periods. At 30 m the measurements give average winds from 6.8 to 7.2 m/s. After long-time corrections the corresponding numbers are 6.1 to 7.1 m/s due to large differences between different methods to correct. At 50 m the measured average wind speed varies between 7.5 and 7.7 m/s. After having applied the long-time corrections 7.0 to 7.5 m/s. Also the observed average gradients differ giving the exponent in the exponential profile relation varying between 0.07 and 0.11.

Comparing with the modeled average wind profile we see that the model results give a larger vertical gradient. At 30 m the model predicts lower average wind speed than the observations give, 5.8 m/s with 100 m grid resolution. The average of the long-time corrected measurement results gives 6.6 m/s – 0.8 m/s higher than the model results show. At 50 m the model results give the average wind speed 6.4 m/s. Here the measurements after long-time corrections give 7.2 m/s – 0.6 m/s above the model results. The difference between model and observations thus decreases with increasing height.

Using the exponential profile relationship to extrapolate the observation to 100 m height, the difference between model and observations is close to zero using the average of the two observational data sets – 7.6 m/s for both. But the difference between the two observations is large – 7.3 and 8.2 m/s – partly due to difference in mean wind speed as such, partly due to different observed vertical wind gradients.

It has not been possible to in more detail judge if one or the other of the two data sets could be more or less reliable. It seems, however, probable that the heated Vaisala anemometers should give more correct results, although it is known that these anemometers also are affected by icing. If this is so, the observed long-time corrected annual average wind speed is more probable to be 6.9 m/s and 7.3 m/s at 50 m and 100 m heights respectively. The model results gives the annual average wind speed of 6.3 m/s and 7.6 m/s at these heights respectively, showing a larger gradient given by the model as compared to the measurements, at least for the current measurement period. But the agreement at 100 m is well within the expected uncertainties both regarding the observations and the model results.

Referenser

Andrén, A., 1990: Evaluation of a turbulence closure scheme suitable for air pollution applications. *J. Appl. Meteor.,* **29,** 224-239.

Bergström, H. and Söderberg, S., 2009: Wind Mapping of Sweden – Summary of results and methods used. Elforsk report 09:04, pp 84.

Bergström, H., 2004: Higher-order closure meso-scale modelling for wind resource estimates in Sweden. Proceedings from EWEC2004, London, November 2004.

Bergström, H. and Lindholm, M., 2003: Higher-order closure meso-scale modelling for wind climate estimates. Proceedings WWEC2003, Cape Town, South Africa, 23-26 Nov. 2003.

Bergström, H., 2002: Boundary-layer modelling for wind climate estimates. *Wind Engineering*, **vol. 25,** No. 5, 289-299.

Bergström, H., 1996: A climatological study of boundary layer wind speed using a meso-γ-scale higher-order closure model. *J. Appl. Meteor.,* **35,** 1291-1306.

Bergström H. and Källstrand K., 2000: Measuring and modelling the wind climate in a mountain valley in northern Sweden. Proceedings, Boreas V, 29 Nov.-1 Dec. 2000, Levi, Finland.

Bergström, H. and Källstrand, B., 2001: Estimating Wind Potential in a Complex Terrain Arctic Mountain Valley. Proceedings EWEC'1001, Copenhagen 3rd - 7th July 2001.

Brooks I. M., Söderberg S. and Tjernström M., 2003: The Turbulence Structure of the Stable Atmosheric Boundary Layer Around a Coastal Headland: Aircraft Observations and Modelling Results.

Burk, S. D., and W. T. Thompson, 1996: The summertime low-level jet and marine boundary-layer structure along the California coast. *Mon.Wea. Rev.,* **124,** 668-686.

Burk, S. D., T. Haack, and R. M. Samelson, 1999: Mesoscale simulation of supercritical, subcritical and transcritical flow along coastal topography. *J. Atmos. Sci.,* **56,** 2780-2795.

Chen, S., J. Cummings, J. Doyle, R. Hodur, T. Holtt, C.S. Liou, M. Liu, J. Ridout. J. Schmidt, W. Thompson, A. Mirin, and G. Sugiyama, 2003: COAMPSTM version 3 model description - general theory and equations. Naval Research Laboratory Technical Report, NRL/ PU7500-04-448. 141 pp.

Enger L., 1990: Simulation of dispersion in a moderately complex terrain. Part A. The fluid dynamic model. *Atmos Environ.,* **24A,** 2431-2446.

Enger L., Koracin, D. and Yang, X., 1993:'A Numerical Study of the Boundary-layer Dynamics in a Mount Valley. Part 1: Model Validation and Sensitivity Experiments', *Boundary-Layer Meteorol.,* **66,** 357-394.

Farr, T. G., et al. (2007), The Shuttle Radar Topography Mission, Rev. Geophys., 45, RG2004, doi:10.1029/2005RG000183.

Hodur, R. M., 1997: The Naval Research Laboratory's Coupled Ocean/Atmosphere Mesoscale Prediction System (COAMPS). *Mon. Wea. Rev.,* **125,** 1414-1430.

Kalnay, E. et al.: 1996: The NCEP/NCAR 40-year reanalysis project, Bull. Amer. Meteor. Soc., 77, 437-470.

Koracin, D. and Enger, L., 1994: A Numerical Study of the Boundary-layer Dynamics in a Mount Valley. Part 2: Observed and Simulated Characteristics of Atmospheric Stability and Local Flows, *Boundary-layer Meteorol.,* **69,** 249-283.

Mellor, G. L., and Yamada, T., 1974: A hierarchy of turbulence closure models for planetary boundary layers, *J. Atmos. Sci.,* **31,** 1791-1806.

Nilsson, E. och Bergström, H., 2009: Från mätt vind till vindklimat – normalårskorrigering. Elforsk Rapport 09:03, 27 sidor.

Pielke, R. A., 1984: *Mesoscale Meteorological Modelling*. Academic Press, 612 pp.

Sandström, S., 1997: Simulations of the Climatological Wind Field in the Baltic Sea Area using a Mesoscale Higher-Order Closure Model, *J. Appl. Meteor.,* **36,** 1541-1552.

Schmith, T., Alexandersson, H., Iden, K.,and Tuomenvirta, H., 1997: North Atlantic – European Pressure Observations 1868-1995 (WASA dataset version 1.0), Danish Meteorological Institute, Technical Report 97-3.

Söderberg, S., and Tjernström M., 2001: Supercritial Channel Flow in the Coastal Atmospheric Boundary Layer: Idealized Numerical Simulations, *J. Geophys. Res.,* **106,** 17811-17829.

Söderberg, S., and Tjernström M., 2002: Diurnal Cycle of Supercritial Along-Coast Flows, *J. Atmos Sci.,* **59,** 2615-2624.

Söderberg, S., and O. Parmhed, 2006: Numerical modelling of katabatick flow over a melting outflow glacier. *Bound.-Layer Meteor.,* **120,** 509-534.